# Investigation of Mechanism and Its Key Factors Associated with Graft Rejection in Allogeneic Corneal Transplantation Using Aqueous Humor Liquid Biopsy

Yong Woo Ji

The Graduate School
Yonsei University
Department of Medicine

# Investigation of Mechanism and Its Key Factors Associated with Graft Rejection in Allogeneic Corneal Transplantation Using Aqueous Humor Liquid Biopsy

A Dissertation Submitted
to the Department of Medicine
and the Graduate School of Yonsei University
in partial fulfillment of the
requirements for the degree of
Doctor of Philosophy in Medical Science

Yong Woo Ji

December 2024

**This certifies that the Dissertation of Yong Woo Ji is approved**

| | |
|---|---|
| Thesis Supervisor | Hyung Keun Lee |
| Thesis Committee Member | Kyoung Yul Seo |
| Thesis Committee Member | Jong Suk Song |
| Thesis Committee Member | Jae Myun Lee |
| Thesis Committee Member | Dongwoo Chae |

**The Graduate School**
**Yonsei University**
**December 2024**

# ACKNOWLEDGEMENTS

Firstly, I would like to express my deepest gratitude to my supervisor, Prof. Hyung Keun Lee, for his unwavering support, patience, and motivation. His guidance, ideas, and immense knowledge were invaluable throughout the course of my PhD. I cannot thank Prof. Lee enough for his mentorship, which brought out the best in me; without his support, this work would not have been possible.

A big thanks to everyone at Severance Eye Research Laboratory for being such wonderful colleagues. In particular, I would like to thank Dr. Chae-Eun Moon, who assisted me on numerous occasions throughout the experiments—your help is greatly appreciated. Thank you to all the other project members for making the lab a lively and inspiring place; it was a pleasure working with each of you.

I extend my sincere thanks to all the members of the Center for Research Facilities at Yonsei University, especially Dr. Dong Young Kang, for your cooperation in Omics analysis. I also want to thank Dr. Kang and Prof. Joon-Ryul Lim for all the laughs and camaraderie we shared.

I would also like to express my appreciation to the Department of Ophthalmology at Severance Hospital for giving me the opportunity to pursue this research. Special thanks to Prof. Kyoung Yul Seo for his expert insights and encouragement throughout my PhD journey.

To my family, I am deeply grateful for your endless support and love. To my mother, who has always believed in me and stood by my side through every challenge, your unwavering faith in my abilities gave me the strength to persevere. To my sisters and their husbands, thank you for your constant encouragement and understanding during my long years of study. Your collective support has been a source of great comfort and motivation, and I am forever thankful for the role you have all played in my journey.

Lastly, I want to extend my deepest appreciation to Juyeon Shin, my soulmate and my unofficial supervisor. Your continuous support, motivation, patience, and sacrifice have been the bedrock of my strength. The countless late nights, the challenges, and the triumphs were all made bearable because of your presence. Your unwavering belief in me, even when I doubted myself, has been my guiding light. Without you by my side, I would not have been able to navigate through the long, often daunting tunnel of this PhD journey. I am profoundly grateful to have you in my life, and I share this accomplishment with you.

December 2024
Yong Woo Ji

# TABLE OF CONTENTS

# LIST OF FIGURES

# LIST OF TABLES

# ABSTRACT

## Investigation of Mechanism and its Key Factors Associated with Graft Rejection in Allogeneic Corneal Transplantation Using Aqueous Humor Liquid Biopsy

**Purpose:** Corneal allograft rejection remains a significant challenge in corneal transplantation, particularly in high-risk patients. Early detection of rejection before clinical manifestations is crucial for improving graft survival. This study aimed to investigate the molecular mechanisms and identify key factors associated with graft rejection in allogeneic corneal transplantation using aqueous humor (AqH) as a liquid biopsy.

**Methods:** A murine model of allogeneic keratoplasty (KP) was used to simulate the immune processes of corneal graft rejection. Comprehensive proteomic and transcriptomic analyses were performed on AqH samples and corneal tissues from different experimental groups, including accepted, transitional, and rejected grafts. Human AqH samples from patients with corneal graft rejection and healthy controls were also analyzed to validate findings from the murine model.

**Results:** Proteomic and transcriptomic analyses revealed distinct molecular profiles corresponding to different stages of graft rejection. Notably, biliverdin reductase B (BLVRB), glutathione peroxidase 1 (GPX1), and cystatin B (CSTB) were significantly upregulated in both murine and human AqH during the transitional and rejection phases. These proteins play pivotal roles in managing oxidative stress and regulating immune responses. BLVRB, GPX1, and CSTB showed potential as early biomarkers for predicting graft rejection before clinical signs appeared.

**Conclusion:** This study demonstrates the utility of AqH as a minimally-invasive liquid biopsy tool for early detection of molecular changes associated with corneal allograft rejection. The identification of BLVRB, GPX1, and CSTB as key biomarkers offers a promising approach for predicting rejection and enabling timely intervention, ultimately improving graft survival outcomes.

---

Key words: Corneal transplantation, Aqueous humor, Biomarkers, Proteomics, Graft rejection, Liquid biopsy, Biliverdin reductase B, Glutathione peroxidase 1, Cystatin B

# I. INTRODUCTION

Allogeneic corneal transplantation, also known as keratoplasty (KP), is a widely practiced surgical procedure aimed at restoring vision in individuals suffering from corneal diseases.[1,2] It is widely acknowledged as one of the most effective solid organ transplantation procedures, largely due to the cornea's unique immune privilege. This characteristic contributes to favorable short- and long-term outcomes and reduces the need for extensive immunosuppressive therapy compared to other organ transplants.[3,4]

However, long-term survival is less promising while the initial success rates for corneal grafts are relatively high. The risk of graft rejection still remains a significant concern, particularly in high-risk patients with inflamed or vascularized corneal beds.[1] In such cases, even with maximal immunosuppressive therapy, the survival rates drop dramatically, with only about 55% of corneal transplants remaining clear after 15 years.[5,6] Repeated KPs are especially vulnerable, with survival rates plummeting with each subsequent procedure, where only 25% of second and 0% of third grafts remain clear after five years.[7]

Despite the significant demand for corneal transplants worldwide, there is a substantial global shortage of donor corneas, with only one cornea available for every 70 required globally.[8,9] South Korea faces similar challenges, where the local supply of donor corneas is insufficient to meet transplant needs, leading to heavy reliance on imported corneal tissues.[10]

## 1.2. The Challenge of Corneal Alloraft Rejection

Corneal allograft rejection is a critical challenge in corneal transplantation, occurring in up to 30% of transplants.[11] This response typically manifests in the form of endothelial rejection, which affects the innermost layer of the cornea responsible for maintaining corneal clarity by regulating hydration.[12] Endothelial rejection is particularly concerning because endothelial cells do not regenerate, leading to graft failure. Other forms of rejection, such as epithelial or stromal rejection, are less common but can occur either alone or in combination.

Early identification of corneal graft rejection is critical for preventing graft failure and ensuring long-term transplant success. The clinical manifestations of rejection can vary depending on the affected corneal layer, but certain signs are indicative of early immune response activation: eye

redness, light sensitivity, foggy vision, and eye pain. Corneal edema may develop, compromising transparency. Sub-epithelial opacities, rejection lines like the Khodadoust line, and raised intraocular pressure further indicate active rejection.

Immunological rejection episodes may occur at any time post-transplant, sometimes even years after surgery, highlighting the importance of long-term graft surveillance. Episodes of rejection can often be reversed if detected early and treated promptly. However, delayed treatment can lead to irreversible damage to the corneal endothelium, making early detection critical for improving graft survival outcomes.

## 1.3. Limitations in Current Diagnostic and Preventive Approaches

While the early detection of graft rejection is crucial for effective intervention, current diagnostic practices rely primarily on clinical examination methods such as slit-lamp biomicroscopy, corneal pachymetry, and specular microscopy.[5,9] However, rejection signs often manifest only after significant damage has occurred, limiting the ability to intervene before irreversible injury to the corneal graft.

Another challenge in corneal transplantation is the limited availability of reliable biomarkers that can predict graft rejection before clinical symptoms appear.[5] There is a significant unmet need for early detection tools that can identify high-risk patients and detect subclinical immune activity. Moreover, current therapies are primarily reactive, targeting rejection episodes only after clinical signs are evident. Long-term use of immunosuppressive agents may cause adverse side effects, including glaucoma, cataract, and opportunistic infections.

The management of high-risk corneal transplants remains particularly difficult. High-risk patients often require more aggressive immunosuppression, and their risk of rejection is higher due to the presence of pre-existing ocular inflammation, corneal vascularization, or multiple prior grafts. Despite advances in surgical techniques, the rejection rates in these patients remain unacceptably high, with some studies reporting failure rates as high as 70% within 10 years.[13]

## 1.4. The Potential of Aqueous Humor as a Diagnostic Biofluid

Aqueous humor (AqH), the clear fluid found in the anterior chamber of the eye, presents a unique opportunity for minimally-invasive diagnostic and monitoring purposes. As a biofluid that directly bathes the corneal endothelium, the AqH is continuously exposed to the cellular and

molecular changes that occur during immune rejection and other pathological processes. Therefore, it has the potential to serve as a valuable source of biomarkers that reflect the underlying immunological state of the transplanted cornea.

The concept of "liquid biopsy" using AqH has garnered increasing interest in recent years, driven by advancements in proteomics and transcriptomics.[14,15] These technologies allow for the comprehensive analysis of proteins, cytokines, and nucleic acids in small volumes of fluid, providing insights into the molecular mechanisms driving rejection. Through proteomic analysis, differentially expressed proteins involved in immune regulation, inflammation, and tissue remodeling can be identified, offering the possibility of detecting early signs of rejection before clinical manifestations occur.

Additionally, analyzing transcriptomic changes in the corneal tissues around AqH may help identify gene expression patterns associated with immune tolerance or activation. By correlating these molecular signatures with clinical outcomes, it is possible to develop a more personalized approach to corneal transplantation, where treatment plans are customized to each patient's risk profile and immune response.

## 1.5. Advances in Proteomics and Transcriptomics for Corneal Graft Rejection Research

Proteomic and transcriptomic analyses have become valuable tools for exploring the molecular mechanisms involved in corneal graft rejection.[14-18] These high-throughput techniques uncover diverse proteins and genes with altered expression during the immune response to allogeneic corneal transplants.

Proteomic analysis has revealed that proteins involved in complement activation, cytokine production, and cell migration are significantly upregulated during rejection, while other proteins that support graft survival may be downregulated.[17,18] These findings offer potential therapeutic targets for modulating the immune response and promoting long-term graft survival. Similarly, transcriptomic analysis of corneal tissues has uncovered key genes involved in immune regulation, energy metabolism, and cytoskeletal reorganization that contribute to graft rejection.[17]

Furthermore, the integration of proteomics and transcriptomics in the analysis of AqH provides a more comprehensive view of the immune processes that occur during rejection.[15] By combining these approaches, researchers can gain a deeper understanding of how proteins and genes interact

to drive the immune response, enabling the discovery of multi-level biomarkers that could improve the accuracy and timeliness of rejection diagnosis.

## 1.6. Previous Research on the Biomarkers for Corneal Allograft Rejection

Previous studies on corneal allograft rejection have greatly advanced our understanding of immune mechanisms. Early research identified T-cell responses and cytokine production, like interleukin-2 and interferon-gamma, as key contributors to rejection, emphasizing Th1-type immune responses in graft failure.[19,20] However, these studies relied heavily on clinical measurments, lacking real-time molecular insights.[21]

Recent molecular advances have focused on identifying biomarkers for early rejection. Proteomic studies with corneal xeno-transplantation have shown upregulation of cytokines, chemokines, and complement proteins like C3a and C5 in rejected grafts, while transcriptomic research highlighted gene expression patterns related to immune activation and inflammation.[17,18] These have opened doors for diagnostic advancement, but clinical application remains limited.

Despite progress, understanding the early molecular changes during rejection remains incomplete. The use of AqH as a minimally-invasive biofluid for detecting these changes is still emerging. Although proteomic and transcriptomic studies have offered valuable insights, translating them into actionable biomarkers for early detection is still challenging. This study builds on existing knowledge by exploring AqH as a real-time diagnostic tool for corneal allograft rejection.

## 1.7. Study Objectives

This study aims to investigate the molecular mechanisms and biomarkers involved in corneal graft rejection using a liquid biopsy approach. By integrating proteomic and transcriptomic analyses of AqH and corneal tissues in murine models of allogeneic transplantation, this research seeks to: 1) Identify early molecular biomarkers in the AqH can predict allograft rejection, enabling timely intervention. 2) Elucidate the different molecular profiles of accepted, transitional, and rejected grafts to track rejection progression. 3) Explore molecular pathways involved in immune responses during rejection to guide future treatment strategies.

# II. MATERIALS AND METHODS

## 2.1. Animal Model of Corneal transplantation

Male C57BL/6 and BALB/c mice (6–8 weeks old) were sourced from Taconic Farms (Hudson, NY) and utilized as donors and recipients, respectively. The mice were housed in a controlled environment with 12-hour light/dark cycles (lights on from 8:00 a.m. to 8:00 p.m.), regulated humidity, and temperature, within a specific pathogen-free facility. Food and water were provided ad libitum throughout the study period. All experimental procedures adhered to the guidelines approved by the Yonsei University Health System Institutional Animal Care and Use Committee (IACUC) and followed the Association for Research in Vision and Ophthalmology Statement for the Use of Animals in Ophthalmic and Vision Research (IACUC approval No. 2018-0270).

The murine KP model has been extensively utilized for decades to study the mechanisms underlying corneal allograft rejection and acceptance.[22,23] Murine orthotopic KP was performed following established protocols.[24-26] Briefly, 2 mm donor corneal buttons were excised from C57BL/6 mice and sutured onto BALB/c recipient corneas following a corresponding 2.0 mm central corneal excision. For syngeneic controls, BALB/c mice served as both donors and recipients. Anesthesia was induced using intraperitoneal injections of ketamine (86.98 mg/kg) and xylazine (13.04 mg/kg). Sterile saline drops were applied to keep the eyes moist throughout the procedure. The grafts were secured with 8 to 10 interrupted 11-0 nylon sutures, which were removed 7 days postoperatively to minimize inflammation. All surgical procedures were performed by a single, experienced, cornea-specialized ophthalmologist (Y. W. Ji), ensuring consistency and precision across all transplantations. Immediately after surgery, topical 0.3% ofloxacin antibiotic (Allergan, Irvine, CA) and 1% prednisolone acetate (Allergan, Irvine, CA) were administered to prevent infection and reduce inflammation. The antibiotic and corticosteroid drops were applied twice daily for the first 7 days postoperatively.

## 2.2. Clinical Evaluation and Experimental Groups

Grafts were evaluated every 3 days for the first 3 weeks and weekly thereafter for up to 6 weeks using slit-lamp bio-microscopy. Corneal photographs were taken using a slit-lamp camera

(Haag-Streit, Köniz, Switzerland) at fixed magnification to ensure consistent image quality across all groups. Graft rejection was defined as corneal opacity that obscured iris details, graded on a scale from 0 (clear) to 5 (fully opaque) (Table 1).[27] Corneal neovascularization was also assessed using an 8-point scale, which measured blood vessel infiltration into the corneal quadrants (Table 2).[27] Graft scoring was conducted by two independent, blinded corneal specialists (Y. W. Ji. and H. K. Lee.), who evaluated the corneal photographs without prior knowledge of the experimental groups or conditions. The scores are presented as the mean ± standard error of the mean (SEM).

**Table 1.** Graft Scorning Based on Corneal Opacity

| Score | Clinical manifestations |
|---|---|
| 0 | Clear |
| 1 | Minimal superficial opacity, iris vessels visible |
| 2 | Minimal stromal opacity, iris vessels visible |
| 3 | Moderate stromal opacity, only pupil margin visible |
| 4 | Intense stromal opacity, only portion of pupil margin visible |
| 5 | Severe stromal opacity, anterior chamber not visible |

**Table 2.** Graft Scorning Based on Corneal Vascularization

| Score | Clinical manifestations |
|---|---|
| 0 | No vessels |
| 1 | Vessels recipient-bed only (1 – 2 quadrants) |
| 2 | Vessels recipient-bed only (3 – 4 quadrants) |
| 3 | Vessels recipient-graft border (1 – 2 quadrants) |
| 4 | Vessels recipient-graft border (3 – 4 quadrants) |
| 5 | Vessels peripheral donor stroma (1 – 2 quadrants) |
| 6 | Vessels peripheral donor stroma (3 – 4 quadrants) |
| 7 | Vessels central donor stroma (1 – 2 quadrants) |
| 8 | Vessels central donor stroma (3 – 4 quadrants) |

Based on clinical observations postoperatively, experimental groups were classified accordingly as follows:

1. **Naïve Control (NC) group**: No surgery, representing the baseline for comparative analysis.
2. **Syngeneic KP-Clear (Syn-C) group**: BALB/c donor corneas were transplanted onto BALB/c recipients, representing clear corneal grafts.
3. **Syngeneic KP-Opaque (Syn-O) group**: BALB/c donor corneas were transplanted onto BALB/c recipients but resulted in opaque grafts.
4. **Allogeneic KP-Accepted (Allo-A) group**: C57BL/6 donor corneas were transplanted onto BALB/c recipients, representing successfully accepted allogeneic grafts without signs of rejection.
5. **Allogeneic KP-Intermediate (Allo-I) group**: C57BL/6 donor corneas were transplanted onto BALB/c recipients that exhibited intermediate graft clarity.
6. **Allogeneic KP-Rejected (Allo-R) group**: C57BL/6 donor corneas were transplanted onto BALB/c recipients that showed complete graft rejection with severe opacity.

## 2.3. Sample Collection in Animal Model

AqH was collected from the KP eyes of anesthetized mice using an anterior chamber perfusion system.[28,29] Briefly, AqH was aspirated from the anterior chamber using a 35-gauge, 5 mm needle (Medicom, Canada) attached to a 10 µl Hamilton syringe with a luer tip under a dissecting microscope. Approximately 3-5 µL of AqH was collected from each eye and immediately frozen at -80°C for proteomic analysis.

After AqH collection, the mice were euthanized, and corneal tissues were harvested for each group. The donor graft and recipient bed were not separated, and the entire corneal button, including both donor and recipient portions, was collected as a single unit. All tissue samples were preserved at -80°C for further analysis including proteomic and transcriptomic studies.

Biological replicates of n=7 mice were used per group for proteomic or transcriptomic analysis, with all samples collected in triplicate to ensure reproducibility of results.

## 2.4. Human Participants and Sample Collection

This study adhered to the ethical principles outlined in the Declaration of Helsinki and Good Clinical Practice Guidelines. It was approved by the Institutional Review Board (IRB) of Yonsei University College of Medicine (Seoul, South Korea; IRB approval No. 3-2017-0361), and written informed consent was obtained from all participants. Participant had no other corneal disease except corneal graft rejection even prior penetrating KP (PKP). Exclusion criteria included patients under 20 years old; those with any ocular history, such as surgery, trauma, infection, allergy, inflammation (e.g., uveitis), glaucoma, or retinal diseases (including macular edema); contact lens users; and individuals with systemic diseases, such as autoimmune conditions, diabetes, or cerebrovascular disease.

We collected AqH biofluids from five patients with corneal graft rejection during re-PKP. Detailed demographic information is provided in Table 1. Normal AqH samples were collected from age- and sex-matched cataract patients during cataract surgery. Approximately 150 μL of AqH was aspirated from the anterior chamber during the procedure. All collected samples were immediately stored at -80°C until analysis.

**Table 3.** Demographic Characteristics of Patients Enrolled in the Present Study

| | **Control (n=7)** | **Rejected (n=7)** |
|---|---|---|
| Age, y | 60.5 ± 6.29 | 57.48 ± 9.21 |
| Sex, n (Female: Male) | 3:4 | 3:4 |

Data are presented as mean ± standard deviation. Comparisons of clinical values between two groups were analyzed using the Wilcoxon signed-rank test.

## 2.5. Proteome Analysis using LC-MS/MS

### 2.5.1. Sample Preparation and In-solution Digestion

Pooled AqH samples from murine models and human participants were used for global profiling with tandem mass tag (TMT) labeling. Protein concentrations were determined in duplicate using the bicinchoninic acid (BCA) assay following the manufacturer's instructions (Thermo Scientific, Foster City, CA, USA). High-abundance proteins were depleted using Seppro IgY spin columns (Sigma Aldrich, St. Louis, MO, USA) to enhance the detection of low-

abundance marker proteins in AqH. Highly abundant proteins were subjected to in-solution digestion to generate peptides.

For peptide preparation, samples were mixed with 10 M urea in 100 mM ammonium bicarbonate (v/v, 1:1), yielding a final urea concentration of at least 5 M, and incubated at room temperature for 30 minutes to facilitate denaturation. Reduction was performed using 10 mM dithiothreitol, followed by alkylation with 30 mM iodoacetamide. Proteins were digested overnight at 37°C with trypsin at a protein-to-protease ratio of 50:1 (w/w). The reaction was stopped with 0.4% trifluoroacetic acid (TFA), and peptides were desalted using a C18 Harvard macro spin column (Harvard Apparatus, Holliston, MA, USA). The purified peptides were then dried and stored at -80°C for further analysis.

For each experimental group, 100 μg of proteins from murine corneal tissues were reduced with 10 mM dithiothreitol for 30 minutes at room temperature, followed by alkylation with 30 mM iodoacetamide for 45 minutes in the dark. Subsequently, the samples were diluted with 100 mM ammonium bicarbonate to achieve a final urea concentration of 2 M. Proteins were enzymatically digested with trypsin and incubated at 37°C for 16 hours. To terminate the reaction, 0.8% trifluoroacetic acid (TFA) was added. The resulting tryptic peptides were then purified using a C18 Harvard macro spin column (Harvard Apparatus) for desalting. The purified peptides were concentrated using a speed vacuum and preserved at -80°C for further analysis.

### 2.5.2. TMT Labeling for Relative Quantification

Desalted peptides from each sample were labeled with 9-plex TMT reagents according to the manufacturer's instructions (Thermo Scientific). Peptides were dissolved in 100 μL of 100 mM triethylammonium bicarbonate, and TMT reagents, prepared in anhydrous acetonitrile as per the optimized protocol, were added. The labeling reaction was carried out for 1 hour at room temperature and quenched with 5% hydroxylamine for an additional 15 minutes of incubation. The TMT-labeled peptides were combined into a single tube and dried using a speed vacuum centrifuge. To achieve separation based on hydrophobicity, the peptides were fractionated into 12 fractions using a High pH reversed-phase peptide fractionation kit (Thermo Scientific). The collected fractions were subsequently dried once more using a speed vacuum and stored until further analysis.

### 2.5.3. Global Profiling using LC-MS/MS

Dried peptide samples were dissolved in 0.1% formic acid prepared using HPLC-grade water and analyzed with a Q Exactive Orbitrap Hybrid Mass Spectrometer connected to an EASY-nLC 1000 system (Thermo Scientific). For global proteomic profiling, a solvent gradient was employed: starting with 5% to 50% of solvent B over 85 minutes, increasing to 80% of solvent B within 1 minute, holding steady for 8 minutes, and finally re-equilibrating the column at 1% of solvent B for 30 minutes (Solvent A: water with 0.1% formic acid; Solvent B: acetonitrile with 0.1% formic acid). Ionization was achieved using a spray voltage of 1.8 kV applied to the column tip. MS1 spectra acquisition was conducted at a resolution of 70,000, with the AGC target set at $1.0 \times 10^6$. The instrument was configured to select the 20 most abundant ions, isolating them with a 2 m/z window, fragmenting them through higher-energy collisional dissociation (HCD) with a normalized collision energy of 30. The resolution for MS2 spectra was maintained at 70,000 for ions at 200 m/z, and a dynamic exclusion time of 30 seconds was applied to avoid repeated ion sampling. Each sample was run in triplicate to ensure reproducibility and minimize technical variation.

### 2.5.4. Processing and Analysis of Proteomic Data

Raw mass spectrometry (MS) files were analyzed using the Proteome Discoverer software (Thermo Scientific) with the SEQUEST HT® search engine for peptide identification. Peptides with a minimum length of six amino acids were considered for identification. Carbamidomethylation was designated as a static modification, whereas oxidation of methionine and acetylation at the protein N-terminus were specified as variable modifications. The digestion parameters were set to recognize trypsin specificity, permitting a maximum of two missed cleavages. The search tolerances were set at 6 ppm for precursor ions and 20 ppm for fragment ions. A false discovery rate (FDR) threshold of 1% was applied to ensure high confidence in protein and peptide identifications. Common contaminants were removed from the dataset. Statistical analyses, including principal component analysis (PCA) and hierarchical clustering with heat mapping, were performed using MetaboAnalyst 5.0, a web-based platform designed for comprehensive statistical evaluation and visualization.

Gene ontology (GO) analysis was conducted using g-Profiler and the Database for Annotation, Visualization, and Integrated Discovery (DAVID) to investigate GO-biological processes (GO-BP)

and GO-cellular components (GO-CC) in corneal tissues and AqH under syngeneic or allogeneic KP conditions, compared to naïve controls. Differentially expressed proteins (DEPs) were used to identify enriched GO terms. Visualization networks of the enriched processes were generated with Cytoscape 3.7.2 software. EnrichmentMap and AutoAnnotate plugins in Cytoscape were utilized to interpret and construct the network, facilitating a comprehensive understanding of the enriched biological pathways and cellular components.

#### 2.5.5. Statistical Analysis

Statistical evaluations were conducted using MetaboAnalyst version 5.0 (Wishart Research Group, Edmonton, Alberta, Canada) and GraphPad Prism version 10 (GraphPad Software Inc., La Jolla, CA, USA). Data normality was tested using the Kolmogorov-Smirnov test. For datasets not conforming to a normal distribution, the Mann-Whitney U test or Wilcoxon signed-rank test was applied. Conversely, one-way analysis of variance (ANOVA) followed by Tukey's post-hoc test or unpaired Student's t-test was utilized for normally distributed datasets to compare group variations. DEPs were defined as those showing more than ±2-fold changes in expression with *P*-values less than 0.05.

### 2.6. Transcriptome Analysis using RNA-sequencing

#### 2.6.1. RNA Preparation and Library Construction

The Quant-IT RiboGreen assay (Invitrogen, Middlesex County, MA, USA) was utilized to quantify total RNA concentration. RNA integrity was evaluated using TapeStation RNA ScreenTape (Agilent Technologies, Santa Clara, CA, USA), and only samples with an RNA Integrity Number (RIN) greater than 7.0 were included in the analysis.

RNA library preparation involved the use of 1 μg of total RNA per sample with the Illumina TruSeq Stranded mRNA Sample Prep Kit (Illumina, Inc., San Diego, CA, USA). Poly-A mRNA was selectively isolated using magnetic beads conjugated with poly-T oligos, followed by fragmentation into smaller sections using divalent cations under elevated temperatures. The fragmented RNA was reverse-transcribed into first-strand cDNA using SuperScript II reverse transcriptase (Invitrogen) and random primers. Second-strand cDNA synthesis was subsequently

performed with DNA Polymerase I, RNase H, and dUTP. The cDNA fragments underwent end-repair, A-tailing, and ligation to sequencing adapters.

The resulting libraries were enriched through PCR amplification, quantified using Kapa Library Quantification Kits specific to Illumina platforms (Kapa Biosystems, Wilmington, MA, USA), and further validated using TapeStation D1000 ScreenTape (Agilent Technologies). Sequencing of the indexed libraries was conducted using the Illumina NovaSeq platform (Illumina, Inc., San Diego, CA, USA) in paired-end mode (2×100 bp reads) at Macrogen, Inc. (Seoul, Korea).

### 2.6.2. Data Analysis of RNA-sequencing

The initial sequencing data were preprocessed to eliminate low-quality reads and adapter sequences before proceeding to downstream analyses. Cleaned reads were aligned to the Mus musculus genome (mm10) using HISAT v2.1.0.[30] HISAT utilizes a combination of global whole-genome and multiple local indexes, constructed using the Burrows-Wheeler transform (BWT) and graph FM index (GFM). This indexing strategy allows HISAT to perform spliced alignments more efficiently than commonly used tools like Bowtie and BWA. The reference genome (mm10) and corresponding annotation files were obtained from the National Center for Biotechnology Information (NCBI).

Reconstruction of known transcripts was performed using StringTie v2.1.3b.[31,32] Transcript and gene expression levels were quantified as read counts or normalized as FPKM (Fragments Per Kilobase of transcript per Million mapped reads) values for each sample. These expression profiles were used to conduct downstream analyses, such as identifying differentially expressed genes (DEGs). DEGs or transcripts across experimental conditions were determined through statistical hypothesis testing.

### 2.6.3. Statistical Analysis

Gene abundances were calculated as read counts using StringTie, and differential expression analyses were conducted to identify DEGs. Genes with read counts of one or fewer across all samples were excluded from analysis. The remaining dataset was transformed using a log2 scale and normalized with the TMM (Trimmed Mean of M-values) method. Statistical significance of

differential expression was determined using the exactTest function in edgeR, which tests fold change under the null hypothesis that no difference exists between groups.[33] Further statistical analyses were performed with GraphPad Prism (version 10.0), and normality was evaluated using the Shapiro-Wilk test. For data following a normal distribution, one-way ANOVA with Tukey's post-hoc test was applied for comparisons between groups, while non-parametric data were assessed using the Mann-Whitney U test. *P*-values were adjusted for multiple comparisons using the Benjamini-Hochberg method to control the FDR. Hierarchical clustering of DEGs was performed using complete linkage with Euclidean distance as the similarity metric. Functional enrichment, annotation, and pathway analyses for significant genes were carried out using gProfiler (https://biit.cs.ut.ee/gprofiler/orth) and the Kyoto Encyclopedia of Genes and Genomes (KEGG) pathway database (http://www.genome.jp/kegg/pathway.html). All visualizations and DEG-related analyses were completed using R software (version 3.6.1).

# III. RESULTS

## 3.1. Clinical Evaluation of Corneal Grafts

Corneal clarity and vascularization were evaluated across the experimental groups following murine KP. Representative corneal photographs (Figure 1A) illustrate the varying levels of opacity and vascularization among the groups. The Naïve Control group exhibited clear, non-operated corneas with no signs of opacity or neovascularization.

In the Syn-C group, the corneas remained transparent with minimal immune response, confirming that syngeneic transplantation did not trigger an immune reaction. However, the Syn-O group showed notable corneal opacity due to surgically induced inflammation, despite the syngeneic nature of the grafts.

In contrast, allogeneic grafts exhibited distinct outcomes based on the degree of immune response. The Allo-A group demonstrated relatively clear corneas, with minimal opacity or vascularization, suggesting that these grafts were accepted with only mild immune activity. In the Allo-I group, moderate corneal opacity and neovascularization were observed, indicating a

transition from acceptance to rejection, where immune surveillance and early immune activation might be occurring. The Allo-R group, as expected, exhibited severe opacity and extensive neovascularization, consistent with full graft rejection.

The Allo-A group showed a higher opacity score compared to the Syn-C group, but a comparable vascularization score (opacity: 1.21±0.24 vs. 0.36±0.18, respectively, $P<0.05$; vascularization: 1.16±0.14 vs. 0.64±0.24, respectively, $P=0.56$). The Allo-R group exhibited the highest rejection scores (opacity: 4.43±0.13; vascularization: 6.00±0.44). The Allo-I group, with intermediate scores, presented a transitional profile. However, there was no statistically significant difference compared to the Syn-O group (opacity: 2.64±0.09 vs. 2.07±0.25, $P=0.24$; vascularization: 3.80±0.45 vs. 3.60±0.54, $P=0.99$) (Figure 1B).

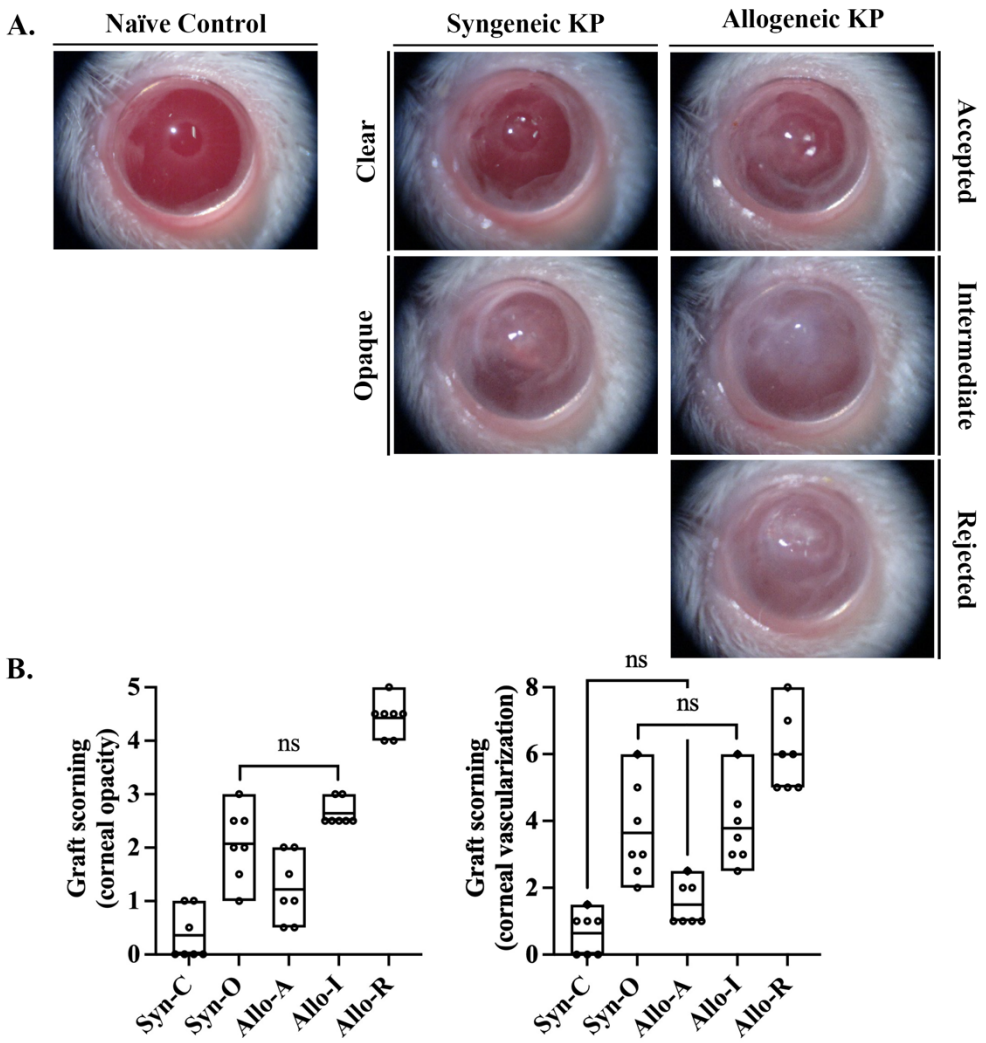


**Figure 1.** Representative Corneal Photographs and Graft Evaluation in the Murine Corneal Transplantation Model

**A.** The photographs illustrate corneal opacity and vascularity across the different groups with keratoplasty (KP), including Naïve Control, Syngeneic KP-Clear (Syn-C), Syngeneic KP-Opaque (Syn-O), Allogeneic KP-Accepted (Allo-A), Allogeneic KP-Intermediate (Allo-I), and Allogeneic KP-Rejected (Allo-R).

**B.** Graft scoring for corneal opacity (left) and corneal vascularization (right) across experimental groups. Corneal opacity scores were assessed using a standardized grading system, and corneal neovascularization was evaluated using an 8-point scale. Individual data points represent each mouse, with the range and mean displayed in box plots. Statistical significance was determined using ANOVA test, with $P<0.05$ considered significant. Statistically significant differences were observed between all groups except between Syn-O and Allo-I (ns, not significant; n= 7/group).

## 3.2. Analysis of Aqueous Humor in Murine Models with Allogeneic Corneal Transplantation

### 3.2.1. Proteomic Alterations in the Aqueous Humor

To further elucidate the molecular mechanisms underlying graft rejection and acceptance in the allogeneic KP models, we conducted a comprehensive proteomic analysis of the AqH. Samples were collected from each experimental group 6 weeks post-transplantation (n=7/group) and analyzed through mass spectrometry-based proteomics (Figure 2A). A total of 1,138 unique proteins were identified across the groups, highlighting the complexity and diversity of the AqH proteome.

The hierarchical clustering analysis (Figure 2B) revealed distinct proteomic patterns that differentiated between the naïve (no KP), syngeneic KP, and allogeneic KP groups. The NC and Syn-C groups exhibited similar clustering, indicating minimal pathophysiological response in the AqH. Interestingly, the Allo-A group formed its own distinct cluster, separate from both syngeneic and naïve groups. This suggests that graft acceptance is not a passive state, but rather involves active immune regulation to maintain corneal clarity and prevent rejection.[34,35] In contrast, the Allo-I and Allo-R groups clustered together, indicating proteomic similarities between these groups. This clustering pattern indicates that the immune response begins to escalate even before full rejection is clinically evident in the Allo-I group.

The PCA further validated these findings (Figure 2C). It demonstrates the separation of these proteomic profiles among groups with PC1 for 90.2% of the variance and PC2 for 6.4%. The NC and syngeneic groups formed distinct clusters from the allogeneic groups. The fact that Allo-A clustered closer to Allo-I than to syngeneic groups suggests that immune activity is necessary for graft acceptance, with some overlap in the molecular pathways seen in transitional rejection. Moreover, the hierarchical clustering and PCA analysis revealed distinct proteomic profiles of AqH between Syn-O and Allo-I, despite their similar clinical manifestations.

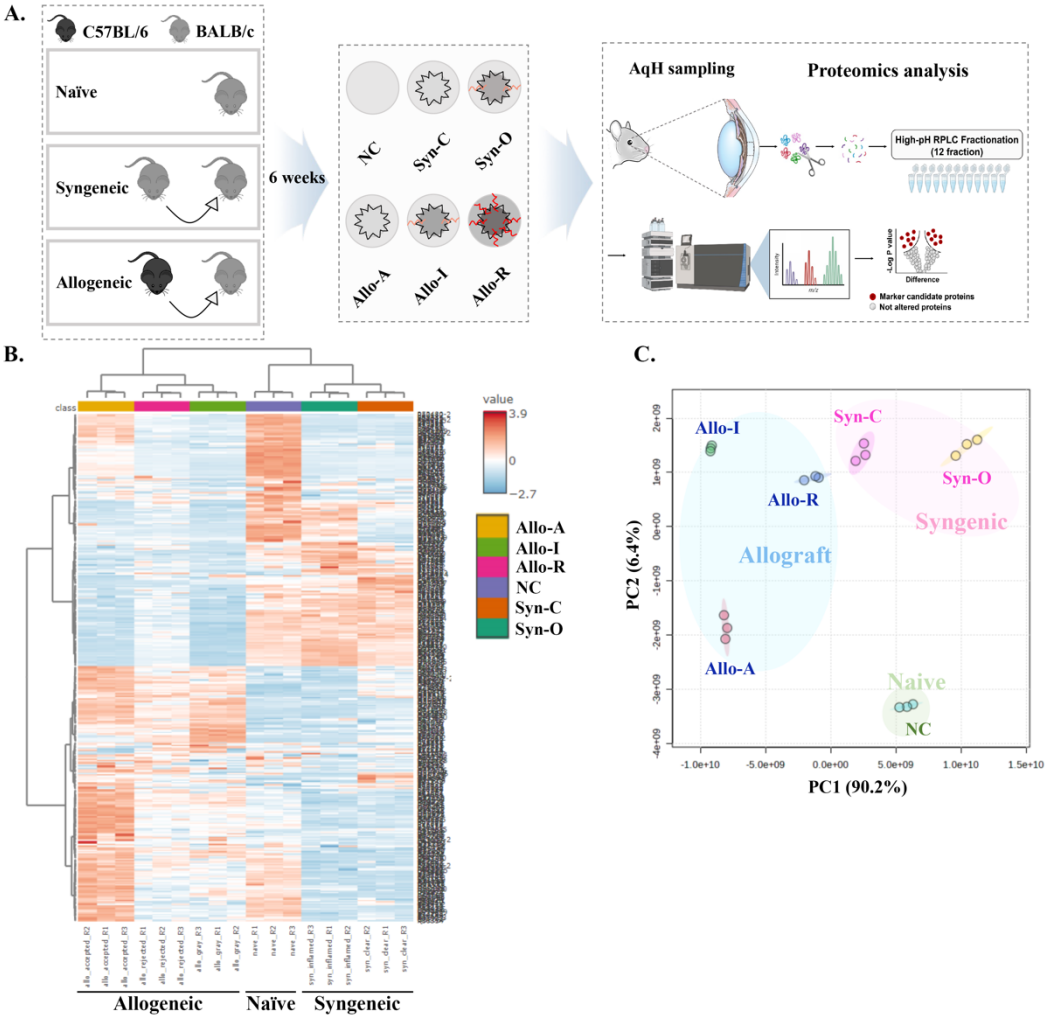


**Figure 2.** Proteomic Analysis of Aqueous Humor in the Murine Corneal Transplantation
**A.** Schematic overview of the experimental design for the proteomic analysis of aqueous humor (AqH) collected from different groups with keratoplasty (KP): Naïve Control (NC), Syngeneic KP-Clear (Syn-C), Syngeneic KP-Opaque (Syn-O), Allogeneic KP-Accepted (Allo-A), Allogeneic KP-Intermediate (Allo-I), and Allogeneic KP-Rejected (Allo-R). The animals were assessed at 6 weeks post-transplantation. AqH was sampled from each mouse and processed through high-pH reverse-phase liquid chromatography (RP-LC) fractionation and analyzed using LC-MS/MS to identify proteomic alterations between the groups (n=7/group).
**B.** Heatmap of hierarchical clustering showing the proteins identified in AqH across three biological replicates for each group. Color gradients in the heatmap correspond to the relative expression levels of proteins, with red indicating upregulation and blue indicating down-regulation.
**C.** Principal component (PC) analysis plot of the proteomic profiles from the AqH samples. The plot shows the separation of experimental groups based on the first two PCs (PC1 and PC2).

### 3.2.2. Differentially Expressed Proteins in the Aqueous Humor

The DEPs were selected in the AqH across the experimental groups by comparing protein expression levels to those in the NC group. The volcano plots (Figure 3A) highlight the DEPs for each group. Proteins with significant fold changes (fold change > 2, *P*-value < 0.05) were selected as DEPs and shown in red (upregulated) or blue (downregulated).

Among the groups, the Allo-I group exhibited the highest number of DEPs (184 proteins), followed by Allo-A (174 proteins), Allo-R (122 proteins), Syn-C (113 proteins), and Syn-O (103 proteins) (Figure 3A). The higher number of DEPs in the Allo-I group suggests dynamic molecular changes, reflecting its transitional immune state between graft acceptance and rejection. Similarly, the Allo-A group showed a considerable number of DEPs, indicating that graft acceptance is associated with active immune regulation.

A hierarchical clustering heatmap (Figure 3B) of significant DEPs demonstrates distinct clustering patterns. The Allo-I and Allo-R groups clustered closely, indicating similarities in immune activation and protein expression. In contrast, the Allo-A group clustered separately from these groups, indicating that successful immune regulation occurs in graft acceptance. The syngeneic groups (Syn-C and Syn-O) formed their own clusters, with Syn-O showing protein alterations primarily associated with surgically-induced inflammation.

The PCA further confirmed the separation of AqH proteomic profiles among the groups as shown Figure 3C. PC1 accounted for 95.9% of the variance, while PC2 captured 3.9%. The allogeneic groups (Allo-I, Allo-R, and Allo-A) formed distinct clusters from the syngeneic groups (Syn-C and Syn-O). Notably, Allo-I and Allo-R were positioned close to each other, reflecting active immune responses in the AqH during graft rejection. In contrast, Allo-A formed a separate cluster, suggesting active immune regulation distinct from the inflammatory responses seen in both the syngeneic and rejecting allografts.

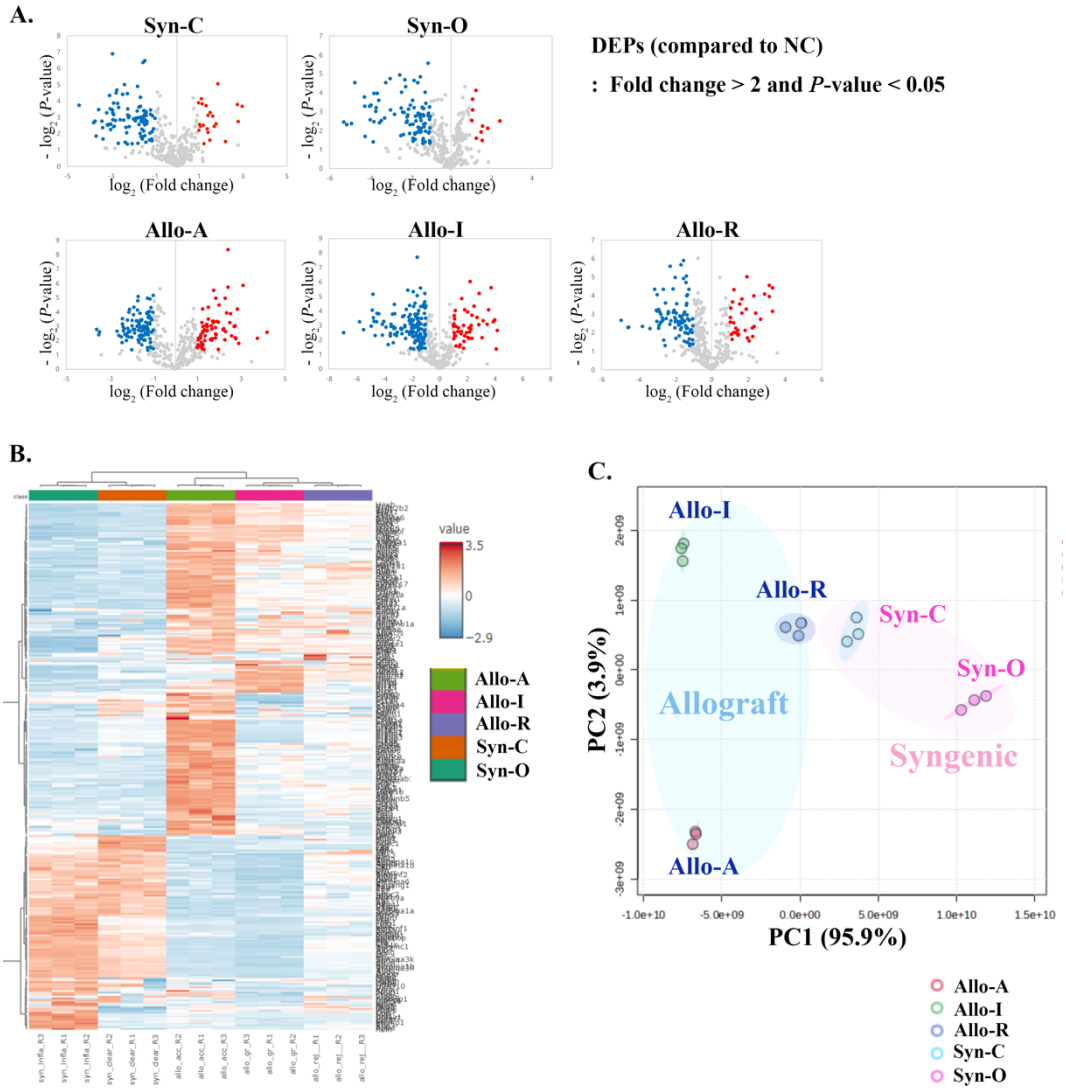


**Figure 3.** Differentially Expressed Proteins in Aqueous Humor Across Experimental Groups
**A.** Volcano plots show differentially expressed proteins (DEPs) for each keratoplasty (KP) group compared to the Naïve Control (NC). Red dots represent upregulated proteins, and blue dots represent downregulated proteins (Fold change > 2 and *P*-value < 0.05). Syn-C = Syngeneic KP-Clear, Syn-O = Syngeneic KP-Opaque, Allo-A = Allogeneic KP-Accepted, Allo-I = Allogeneic KP-Intermediate, Allo-R = Allogeneic KP-Rejected.
**B.** Heatmap showing hierarchical clustering of DEPs across the groups.
**C.** Principal component analysis of proteomic data shows the distinct clustering of the experimental groups. The plot shows the separation of experimental groups based on the first two PCs (PC1 and PC2).

### 3.2.3. Biological Characteristics of Differentially Expressed Proteins in Aqueous Humor

#### 3.2.3.1. Gene Ontology Analysis of Allogeneic-specific Proteins in Aqueous Humor

To explore the biological processes associated with graft rejection and acceptance, Gene Ontology analysis was performed on the DEPs identified in the AqH from both syngeneic (Syn-C, Syn-O) and allogeneic (Allo-A, Allo-I, Allo-R) groups. The Venn diagram in Figure 4A illustrates the overlap and distinctions of DEPs between these KP groups. Across the allogeneic KP groups, a total of 241 DEPs were identified. Of these, 97 DEPs were shared between the syngeneic and allogeneic groups, while the allogeneic groups exhibited 144 unique DEPs, accounting for approximately 60% of the total DEPs in the AqH. This indicates that the immune processes involved in allograft rejection are distinct from those in syngeneic transplants.

Within the allogeneic groups, the Allo-I group exhibited the highest number of unique DEPs (55 proteins, approximately 30% of the total DEPs), reflecting its dynamic immune environment. In contrast, the Allo-A group had 34 unique DEPs (19%) and the Allo-R group had 10 unique DEPs (8%), suggesting that immune regulation in the Allo-A group involves specific biological processes that differ from both rejection and quiescence. Interestingly, 72 DEPs were shared across all allogeneic groups, pointing to common biological pathways activated regardless of graft outcome (Supplementary Figure 1).

Next, a GO-BP network analysis (Figure 4B) of these allogeneic-specific DEPs revealed significant enrichment in processes related to immune response, such as complement activation, cytokine-mediated signaling, and phagocytosis. These processes are central to mediating graft rejection, as they involve both innate and adaptive immune responses aimed at targeting the foreign graft tissue. In particular, complement activation and interleukin-1β production were prominent in both the Allo-I and Allo-R groups, highlighting their role in the progression of rejection. Phagocytic activity was also upregulated, emphasizing the importance of immune cell activation mechanisms in the rejection process.

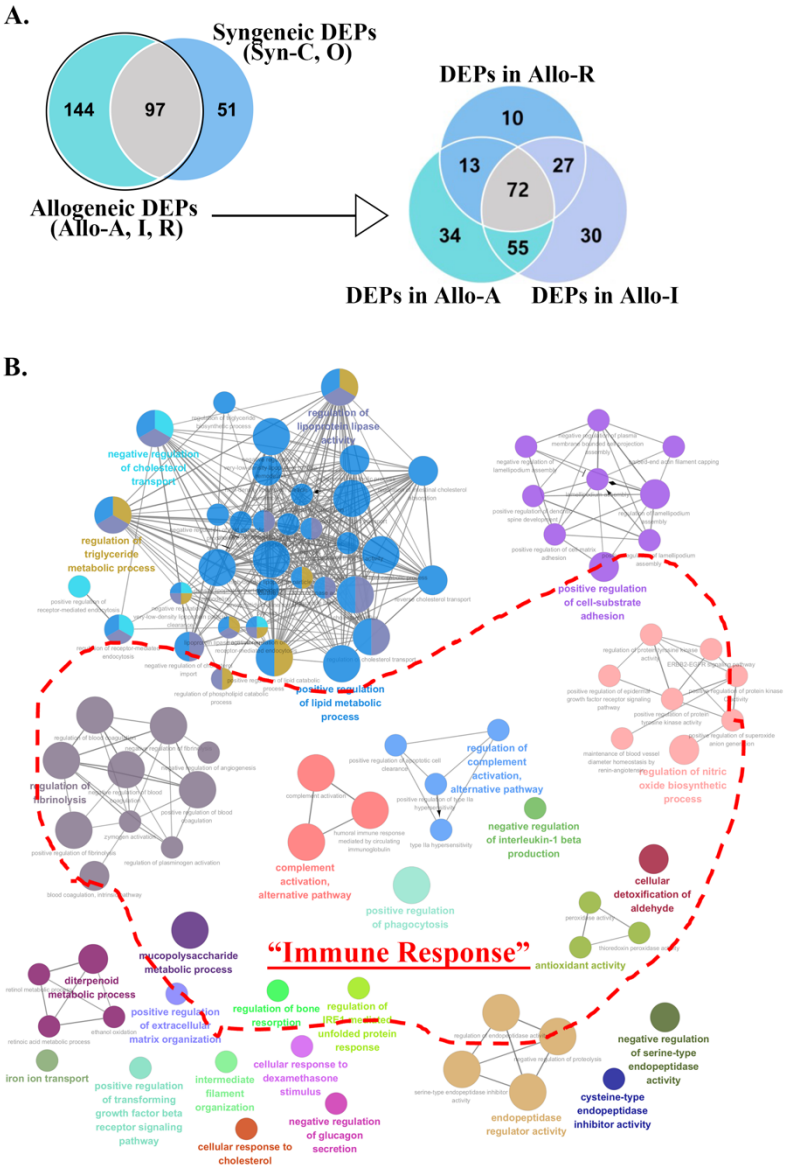


**Figure 4.** Biological Pathway Networks of Differentially Expressed Proteins in Allogeneic Aqueous Humor

**A.** Venn diagrams illustrating the overlap and distinction of differentially expressed proteins (DEPs) between the syngeneic keratoplasty (KP) groups (Syn-C and Syn-O) and the allogeneic KP groups (Allo-A, Allo-I, and Allo-R).

**B.** Gene Ontology (GO) biological process network analysis of DEPs in the allogeneic KP groups. Each node represents an enriched biological process, with node size proportional to the number of proteins involved in the process.

### 3.2.3.2. Gene Ontology Analysis of Proteins Specific to Allogeneic Acceptance in Aqueous Humor

To investigate the biological processes underlying graft acceptance, GO-BP analysis was conducted on DEPs identified in the AqH from the Allo-A group. The analysis revealed both upregulated and downregulated processes, highlighting the molecular pathways involved in maintaining immune tolerance during allogeneic transplantation.

Figure 5A illustrates the upregulated biological processes in the Allo-A group. Several immune-modulatory processes were enriched, particularly those involved in the cellular response to IL-6 and the negative regulation of IL-1β production. These pathways suggest that IL-6 plays a role in controlled inflammation, supporting immune tolerance without leading to rejection. Simultaneously, the suppression of pro-inflammatory signals, such as IL-1β, indicates a reduction in inflammatory responses, contributing to graft stability. Additionally, processes related to hyaluronan biosynthesis and mucopolysaccharide metabolism were upregulated, suggesting active tissue repair and extracellular matrix maintenance during graft acceptance.

Conversely, Figure 5B shows the downregulated biological processes, including the negative regulation of blood coagulation and the alternative complement pathway, indicating reduced immune activation. These downregulated processes suggest that suppression of pro-inflammatory and coagulative pathways is crucial for maintaining a non-rejecting environment. Downregulation of lipid metabolism-related pathways further emphasizes the regulatory shifts occurring during graft acceptance.

Moreover, protein-protein interaction (PPI) network analysis of DEPs unique to the Allo-A group compared to the Naïve control (Figure 6) revealed key regulatory interactions. The network demonstrated downregulation of several immune-related proteins associated with complement activation, including C3 (Complement component 3), C5, C8, and CFB (Complement factor B) (blue nodes). At the same time, proteins involved in inflammatory response, such as NF-kB (Nuclear factor kappa-light-chain-enhancer of activated B cells) and CAMP (Cathelicidin antimicrobial peptide), were upregulated (red nodes). Proteins related to cell localization processes, such as KRT5 (Keratin 5)and S100A6 (S100 calcium-binding protein A6), were also upregulated, suggesting ongoing cellular processes that help maintain immune regulation without triggering rejection.

Proteins related to homeostasis including SERPINF1 (Serpin family F member 1) and PCSK1N (Proprotein convertase subtilisin/kexin type 1 inhibitor) were downregulated, indicating a controlled

reduction of these processes during graft acceptance. Proteins involved in visual system development such as KERA (Keratocan) and CRYG (Crystallin gamma) were also downregulated, reflecting tissue-specific changes contributing to maintaining graft integrity (Figure 6).

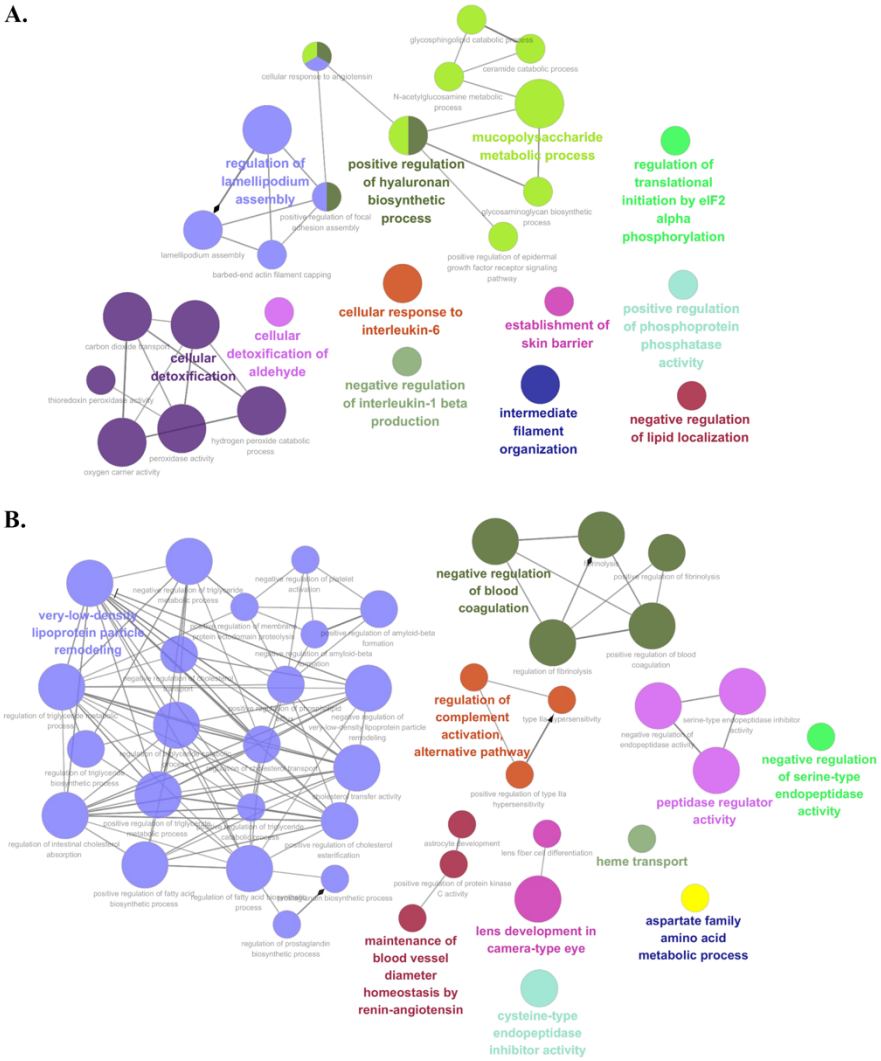


**Figure 5.** Gene Ontology Biological Process of Upregulated and Downregulated Proteins Specific to Allogeneic Acceptance in Aqueous Humor

**A.** Gene Ontology biological process (GO-BP) network analysis of upregulated differentially expressed proteins (DEPs) in the allogeneic keratoplasty-accepted (Allo-A) group.

**B.** GO-BP network analysis of downregulated DEPs in the Allo-A group.

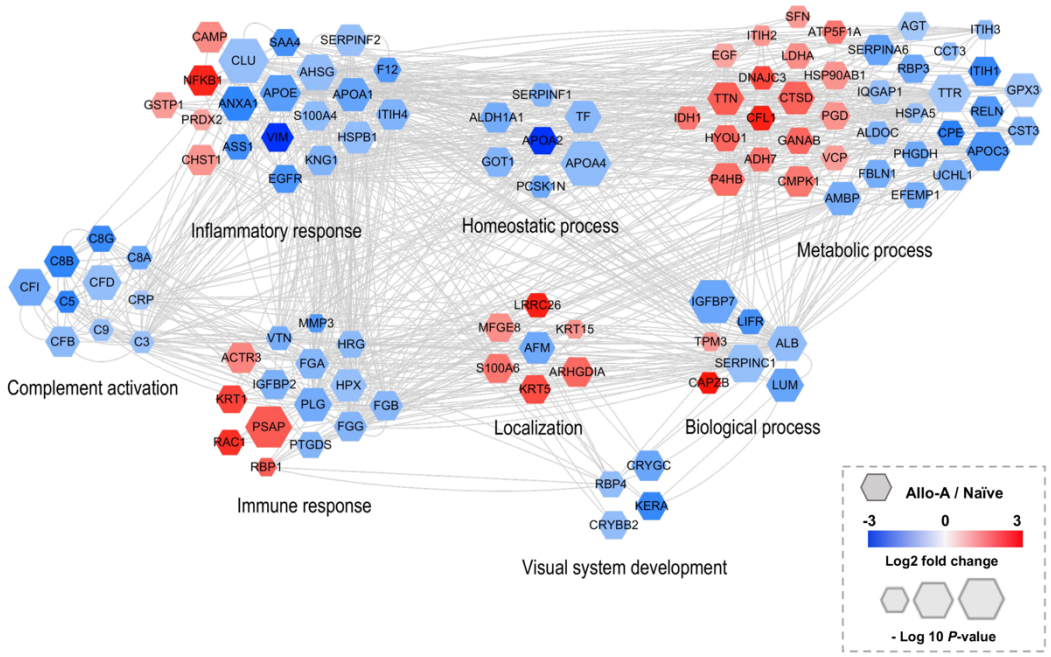


**Figure 6.** Protein-Protein Interaction Network of Proteins Specific to Allogeneic Acceptance in the Aqueous Humor

This figure shows the protein-protein interaction network of differentially expressed proteins (DEPs) in the allogeneic keratoplasty-accepted (Allo-A) group compared to the Naïve Control. The size of the hexagons corresponds to the statistical significance of the interactions, with larger hexagons representing higher significance (measured by -log10 P-value). The color of each hexagon represents the direction of expression: blue indicates downregulated DEPs, and red indicates upregulated DEPs (based on log2 fold change).

### 3.2.3.3. Gene Ontology Analysis of Proteins Associated with Transitional Allogeneic Response in the Aqueous Humor

The analysis of upregulated and downregulated DEPs in the AqH of the Allo-I group highlights multiple immune processes reflective of the transitional phase between graft acceptance and rejection. These findings suggest that ongoing immune activity is preparing the graft for potential rejection as it shifts from a stable state.

GO-BP analysis (Figure 7A) identifies several immune and metabolic processes active during this phase. The upregulated processes include ‘peroxidase activity’ and ‘intermediate filament organization,’ which suggest cellular restructuring and oxidative stress response. The ‘cellular response to interleukin-6’ process, also significantly upregulated, pointing to the central role of IL-6 in modulating immune responses during this transition.

Conversely, the downregulated DEPs (Figure 7B) reveal processes that are actively suppressed during this phase. The reduced ‘acute inflammatory response to antigenic stimulus’ and ‘prostaglandin metabolic process’ suggest a dampened inflammatory state, while the downregulation of ‘peptidase activity’ and ‘triglyceride metabolic process’ reflects shifts in metabolic regulation. Additionally, the downregulation of ‘blood coagulation’ implies an active suppression of pathways that could otherwise exacerbate inflammation or lead to vascular complications.

The PPI network analysis (Figure 8) further delineates the molecular interactions within the Allo-I group, highlighting the balance between immune activation and suppression during this transitional phase. Key immune-related proteins such as RAC1 (Ras-related C3 botulinum toxin substrate 1), which promotes immune cell migration, and CSTB (Cystatin B), a protease inhibitor known to regulate immune responses, were upregulated, contributing to the controlled immune activity observed.

Inflammatory response proteins such as CLU (Clusterin), SERPINF2 (Serpin family F member 2), and GPX1 (Glutathione peroxidase 1) were differentially regulated, confirming the presence of inflammation, though not at the levels typically associated with full rejection. Proteins involved in oxidative stress responses, such as P4HB (Prolyl 4-hydroxylase subunit beta) and BLVRB (Biliverdin reductase B), were also upregulated, reflecting the ongoing cellular stress response. At the same time, homeostasis-related proteins such as APOA1 (Apolipoprotein A1) and ALB (Albumin) were downregulated, suggesting that metabolic regulation is finely tuned in response to

immune activation. Complement components, including C3 and C8a, were suppressed, further indicating that the immune response in the Allo-I group remained regulated, not yet progressing to full rejection (Figure 8).

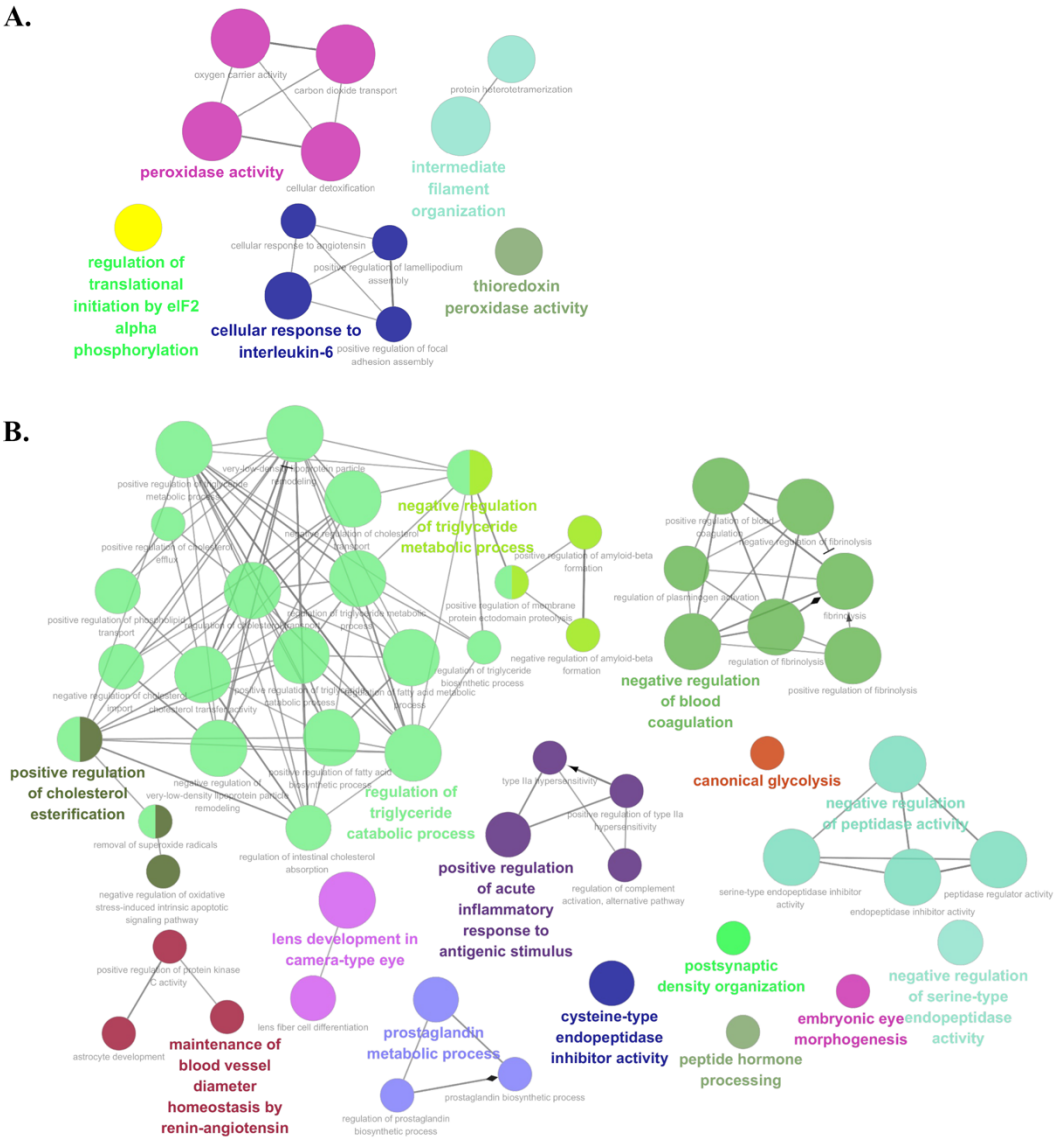


**Figure 7.** Gene Ontology Biological Process of Upregulated and Downregulated Proteins Associated with the Transitional Allogeneic Response in the Aqueous Humor

**A.** Gene Ontology Biological Process (GO-BP) network analysis of upregulated differentially expressed proteins (DEPs) in the aqueous humor (AqH) of the allogeneic keratoplasty-intermediate (Allo-I) group.

**B.** GO-BP network analysis of downregulated DEPs in the AqH of Allo-I group.

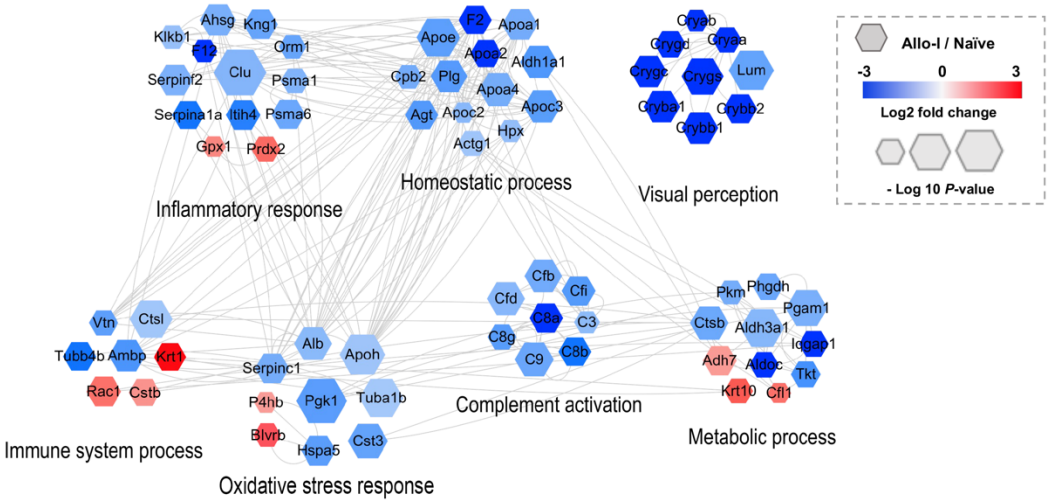


**Figure 8.** Protein-Protein Interaction Network of Proteins Associated with the Transitional Allogeneic Response in the Aqueous Humor

The network illustrates the interactions between differentially expressed proteins in the aqueous humor of the allogeneic keratoplasty-intermediate (Allo-I) group compared to the Naïve Control. Blue hexagons represent downregulated proteins, and red hexagons represent upregulated proteins, with the color intensity corresponding to the fold change (Log2 fold change). The size of the hexagons corresponds to the statistical significance of the interactions, with larger hexagons representing higher significance (measured by -log10 *P*-value).

### 3.2.3.4. Gene Ontology Analysis of Proteins Specific to Allogeneic Rejection in Aqueous Humor

To explore the biological processes driving graft rejection, we analyzed the DEPs from the AqH of the Allo-R group, representing late-stage immune rejection in corneal transplants.

Figure 9A demonstrated the upregulated processes predominantly related to heightened immune activation and inflammatory responses following full-blown graft rejection. Notably, ‘peroxidase activity’ and ‘cellular response to interleukin-6’ were significantly upregulated, indicating the involvement of oxidative stress and pro-inflammatory cytokines like IL-6 during the rejection process. Additionally, processes such as ‘lamellipodium assembly’ and ‘intermediate filament organization’ were enriched, suggesting cytoskeletal changes that facilitate immune cell migration during rejection.

In contrast, Figure 9B revealed key downregulated processes that suggest a suppression of regulatory and metabolic pathways. ‘Prostaglandin metabolic process’ and ‘protein activation cascade’ were downregulated, reflecting a reduced capacity to modulate inflammation and promote tissue repair. The ‘negative regulation of blood coagulation’ points to impared control hemostasis. Additionally, the downregulation of cellular response to reactive oxygen species and positive regulation of CoA-transferase activity indicated a reduced cellular defense against oxidative stress and disruptions in metabolic pathways during rejection.

Next, we generated a PPI network using DEPs from the AqH of the Allo-R group (Figure 10). In the oxidative stress response cluster, BLVRB was upregulated, managing the cellular stress associated with immune activity during rejection. The inflammatory response cluster included upregulated proteins such as GPX1 and PRDX2 (Peroxiredoxin-2), supporting the activation of oxidative damage control mechanisms during rejection. Furthermore, CSTB, involved in the immune response, was upregulated, highlighting its role in preventing excessive tissue degradation while immune cells attack the graft. Localization proteins, such as YWHAB (Tyrosine 3-monooxygenase/tryptophan 5-monooxygenase activation protein beta), MUP4 (Major urinary protein 4) and MUP5, were also upregulated. Those may reflect potential alterations in immune signaling pathways and cellular organization in response to the rejection process. In contrast, several crystallins were downregulated, indicating a loss of structural integrity of the cornea. Their downregulation is likely contributing to the cornea opacity and degradation observed in the rejected grafts.

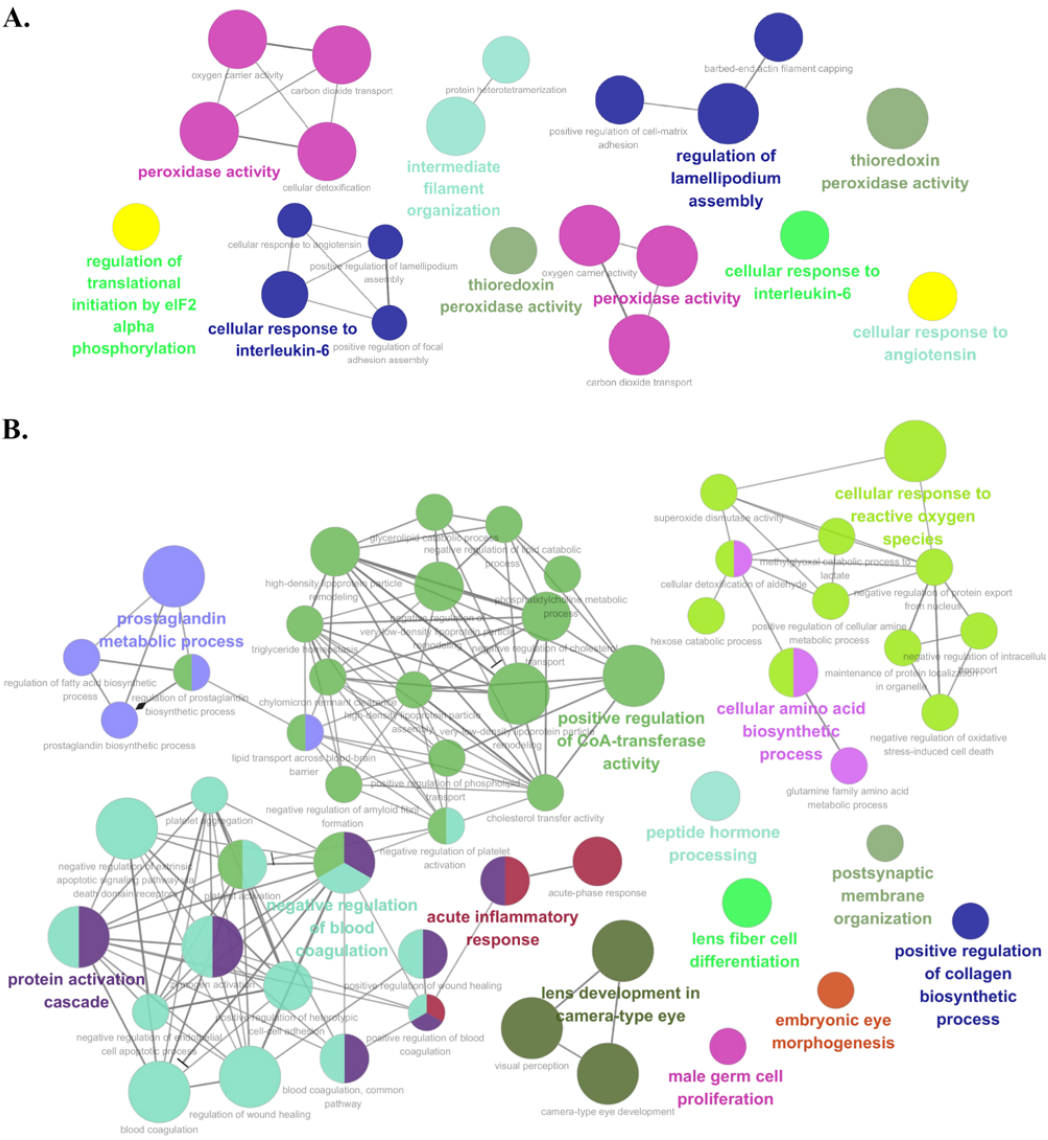


**Figure 9.** Gene Ontology Biological Processes of Differentially Expressed Proteins in the Aqueous Humor of Allogeneic Rejection

**A.** Gene ontology biological pathway (GO-BP) analysis of upregulated differentially expressed proteins (DEPs) in the aqueous humor (AqH) of the allogeneic keratoplasty-rejected (Allo-R) group.

**B.** GO-BP analysis of downregulated DEPs in the Allo-R group.

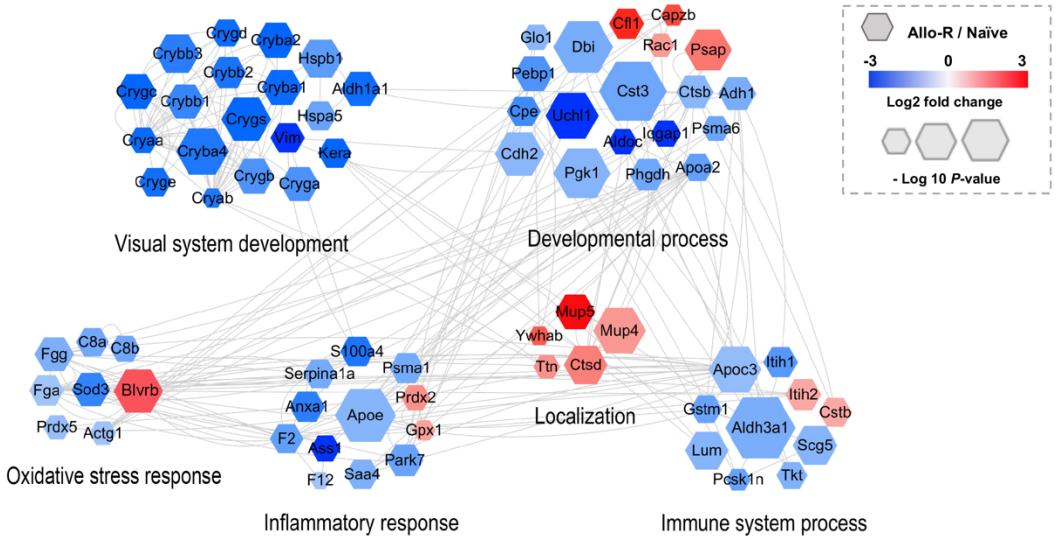


**Figure 10.** Protein-Protein Interaction Network of Proteins Specific to Allogeneic Rejection in the Aqueous Humor

The protein-protein interaction network highlights differentially expressed proteins in the aqueous humor of the allogeneic keratoplasty-rejected (Allo-R) group. Nodes represent individual proteins, and edges represent known interactions between them. The node colors indicate log2 fold change in expression relative to the naïve control group, with red representing upregulated proteins and blue representing downregulated proteins. The size of the nodes correlates with the statistical significance of the expression change (−log10 *P*-value).

### 3.2.3.5. Aqueous Humor Biomarker Candidates for Predicting Corneal Allograft Rejection

To identify potential biomarkers that can predict corneal allograft rejection, we analyzed proteins uniquely present in the Allo-I and Allo-R groups but absent in the Allo-A group. These proteins are likely involved in the early immune response leading to graft rejection, as their expression increases as immune tolerance begins to break down.

The heatmap in Figure 11 illustrates the distinct DEPs in the AqH of the Allo-I and Allo-R groups. Notably, BLVRB (biliverdin reductase B), GPX1 (glutathione peroxidase 1), and CSTB (cystatin B) were consistently upregulated during both the transitional and rejection phases. These proteins play crucial roles in immune modulation and oxidative stress processes, suggesting their potential involvement in the early stages of rejection. Specifically, BLVRB is known for its role in mitigating oxidative damage through its antioxidant activity, indicating an active cellular response to oxidative stress during immune activation. Similarly, GPX1, a key antioxidant enzyme, highlights the ongoing efforts to control oxidative damage during the rejection process. CSTB, a protease inhibitor, regulates proteolysis, which helps balance immune responses and prevents excessive tissue degradation during rejection.

Conversely, several proteins related to normal cellular functions, such as metabolic regulation and tissue homeostasis, were downregulated in the Allo-I and Allo-R groups. ACTG1 (actin gamma 1), PGK1 (phosphoglycerate kinase 1), Cryaa, Cryab, and Crybb1, which are associated with maintaining lens and corneal transparency and providing cellular protection under stress, showed decreased expression. This downregulation suggests a loss of tissue integrity and the inability of the graft to maintain structural resilience, contributing to graft failure and rejection.

The consistent absence of these DEPs in the Allo-A group indicates that their presence in the AqH during the ongoing rejection process is closely associated with the breakdown of immune tolerance. The upregulation of oxidative stress-related and immune-regulatory proteins serves as early molecular signals, potentially allowing for the prediction of rejection before clinical manifestations emerge.

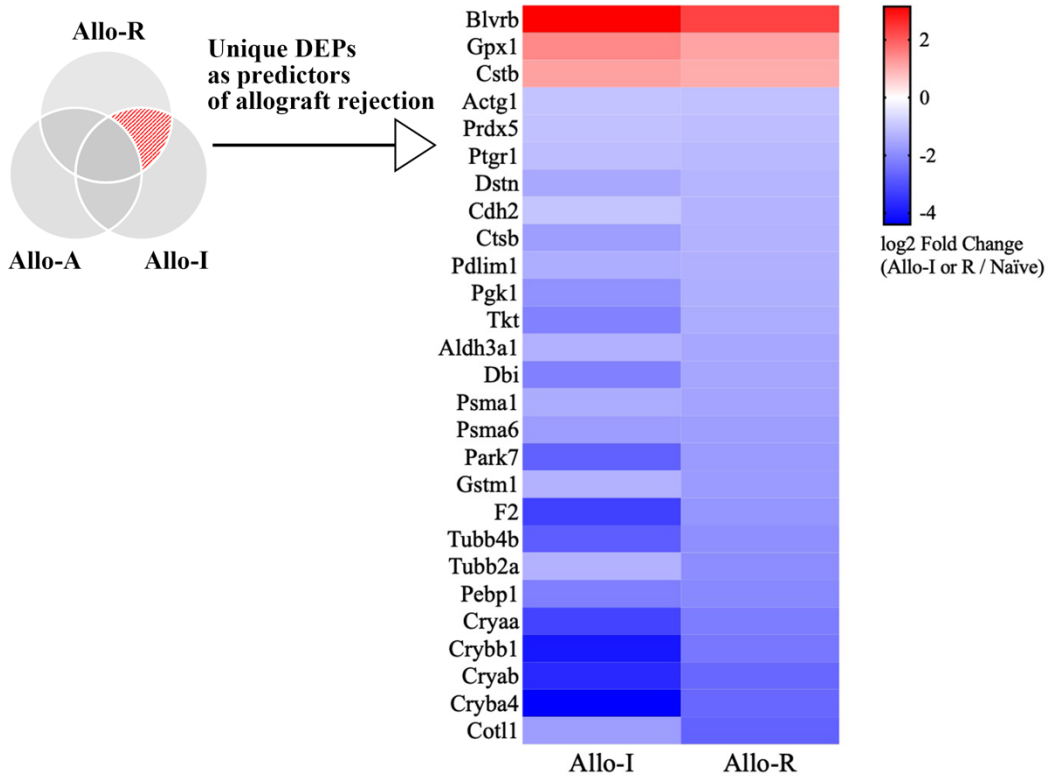


**Figure 11.** Candidate Aqueous Humor Biomarkers for Predicting Corneal Allograft Rejection
This heat map illustrates the differentially expressed proteins (DEPs) unique to the allogeneic keratoplasty-intermediate (Allo-I) and -rejected (Allo-R) groups, even not present in the Allo-accepted (Allo-A) group. Proteins in the heat map are presented according to their log2 fold change (Allo-I or Allo-R vs. Naïve control), with red indicating upregulation and blue indicating downregulation.

## 3.3. Validation of Aqueous Humor Biomarker Candidates in Human Corneal Allograft Rejection through Proteomic Analysis

### 3.3.1. Proteomic Alterations in Human Aqueous Humor

Following the identification of potential biomarker candidates in the murine model, we performed a proteomic analysis of AqH from human patients to assess whether the same proteins could serve as biomarkers for corneal allograft rejection in clinical settings. AqH samples were collected from patients with rejected corneal grafts (n=7) and control patients (n=7) with no signs of rejection. This analysis aimed to validate the relevance of murine biomarker candidates in human samples (Figure 12A).

A total of 833 proteins were identified from the human AqH samples, and there were 106 significantly increased proteins and 66 significantly decreased proteins in patient samples with with rejected corneal allografts, compared to controls (Figure 12B). The volcano plot illustrates the DEPs between the two groups, with significantly upregulated and downregulated proteins (fold change > 2, P-value < 0.05) in the rejected group compared to controls. Consistent with findings from the murine model, BLVRB (biliverdin reductase B), GPX1 (glutathione peroxidase 1), and CSTB (cystatin B) were significantly upregulated in the AqH of human patients with rejected graft.

The heatmap in Figure 12C illustrate the hierarchical clustering of DEPs between the control group and the group with rejected corneal allografts. It provides a clear visual representation of the proteomic changes in AqH during graft rejection. Proteomic profiling revealed distinct expression patterns, with the rejected group showing both upregulated and downregulated proteins compared to the control group. Importantly, the consistency in the rejected group's protein expression profiles indicates common biological pathways activated in the rejection process.

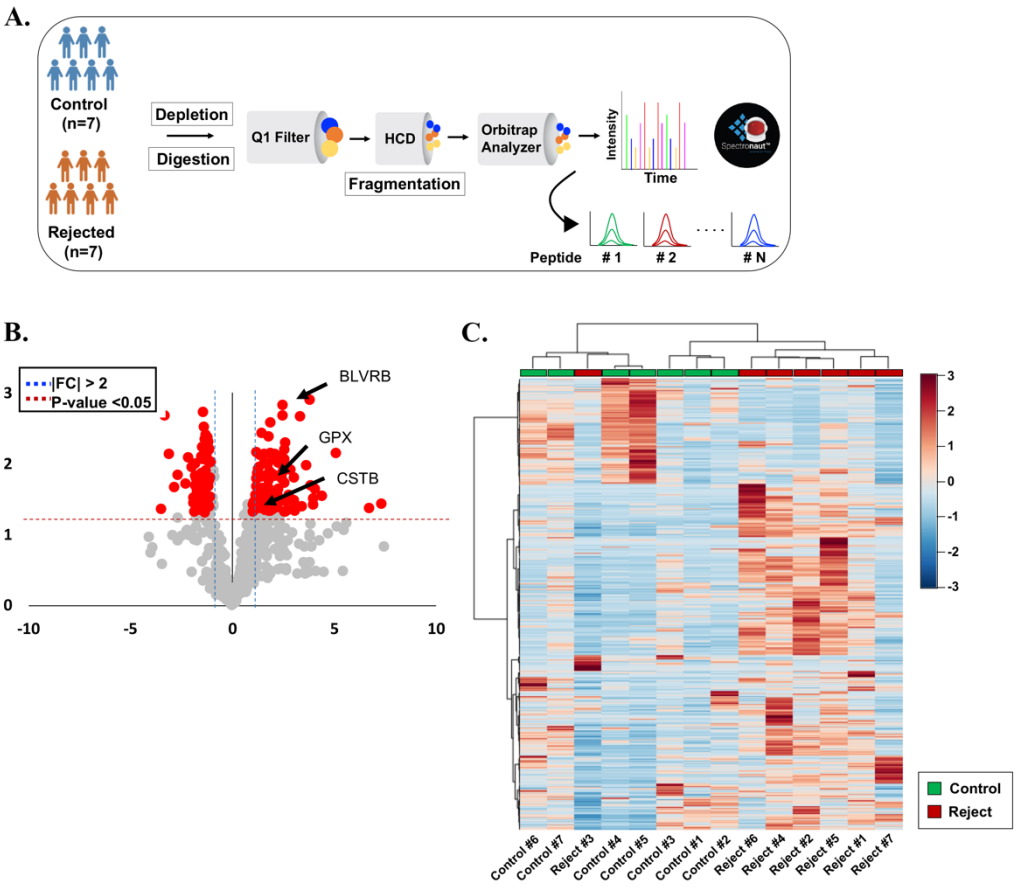


**Figure 12.** Validation of Aqueous Humor Biomarker Candidates in Human Corneal Allograft Rejection through Proteomic Analysis

**A.** Overview of the experimental workflow used for proteomic analysis of human aqueous humor (AqH) samples from control (n=7) and rejected (n=7) corneal graft patients. AqH samples underwent depletion, digestion, and subsequent analysis using high-resolution Orbitrap mass spectrometry.

**B.** Volcano plot displaying the difference in protein expression in human AqH between the two groups. Red dots represent significantly up- and down-regulated proteins (Fold change > 2 and *P*-value < 0.05). Three AqH proteins were identified as markers for predicting corneal allograft rejection, based on AqH proteomics.

**C**. Heatmap showing hierarchical clustering of differentially expressed proteins (DEPs) of AqH in control versus rejected corneal graft group.

### 3.3.2. Protein-Protein Interaction Network in Human Aqueous Humor

To further explore the interactions between these DEPs, a PPI network was constructed based on the DEPs identified in the human AqH samples (Figure 13). This network highlighted several protein clusters involved in key biological processes such as immune response, oxidative stress, and inflammatory regulation.

Importantly, consistent with the findings from the murine model, BLVRB (biliverdin reductase B), GPX1 (glutathione peroxidase 1), and CSTB (cystatin B) were significantly upregulated in the AqH of rejected graft patients. BLVRB and GPX1 were upregulated in the oxidative stress response cluster, mitigating oxidative damage during graft rejection. PRDX2, another oxidative stress-related protein, was also upregulated, suggesting enhanced antioxidant defense mechanisms in response to rejection.

In the immune response cluster, CSTB was upregulated along with complement proteins such as C9 and C1R. CSTB, a protease inhibitor, was also elevated, which is consistent with its role in preventing excessive tissue degradation by modulating immune response. These proteins are part of the complement cascade, which plays a crucial role in immune-mediated tissue damage during rejection. Additionallly, the inflammatory response cluster included upregulated proteins such as SERPINC1 (Serpin family C member 1) and VTN (vitronectin), both of which are involved in modulating inflammation and coagulation.

Other proteins related to developmental processes and cellular communication, such as crystallins, VCAM1 (vascular cell adhesion molecule 1) and DKK3 (dickkopf-related protein 3), were differentially up- or down-expressed.

In summary, this proteomic analysis of human AqH samples aligns with findings from the murine model, validating BLVRB, GPX1, and CSTB as potential biomarkers for corneal allograft rejection. Additionally, other proteins involved in immune response, oxidative stress, and inflammation were differentially expressed, providing further insights into the molecular mechanisms underlying graft rejection. These results support the potential of AqH proteomics in predicting and monitoring rejection in clinical settings.

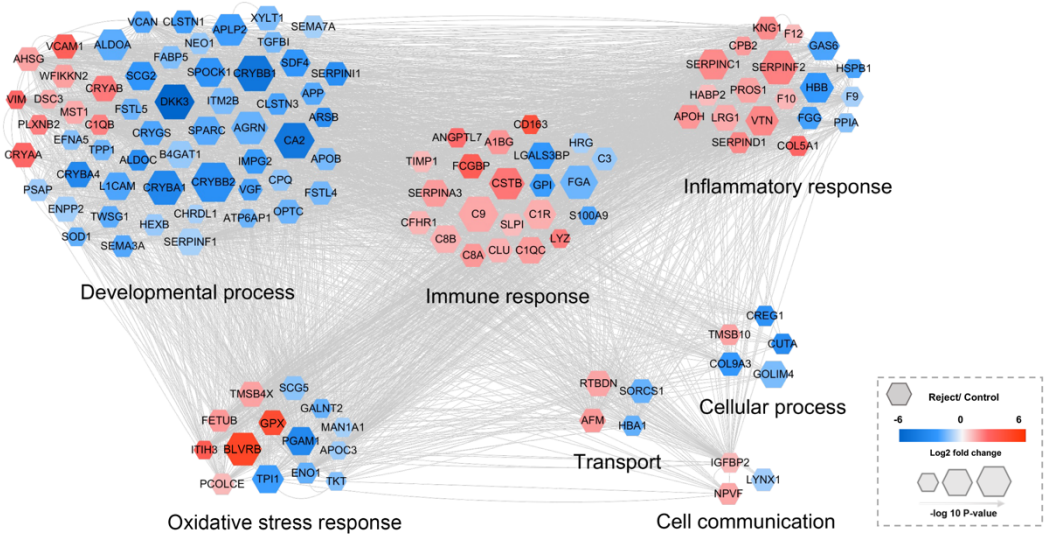


**Figure 13.** Protein-Protein Interaction Network of Aqueous Humor Proteins in Patients with Corneal Allograft Rejection

The protein-protein interaction network showing differentially expressed proteins and significantly enriched biological processes in the aqueous humor of patients with corneal allogeneic graft rejection. Nodes represent individual proteins, and edges represent known interactions between them. The node colors indicate log2 fold change in expression relative to the control group, with red representing upregulated proteins and blue representing downregulated proteins. The size of the nodes correlates with the statistical significance of the expression change (−log10 *P*-value). The connection between nodes (grey lines) indicates either a regulatory role or physical interaction between proteins.

# IV. DISCUSSION

This study aimed to investigate the molecular mechanisms underlying corneal allograft rejection, identifying key proteins in the AqH that can serve as potential biomarkers for early detection of graft rejection. Through comprehensive proteomic analysis of both murine models and human patients, we identified key immune-related and oxidative stress-related proteins, which are consistently upregulated during the transitional and rejection phases. Particularly, BLVRB, GPX1, and CSTB as biomarker candidates for corneal allograft rejection represents a significant step toward improving early detection and management of this condition. These findings provide valuable insight into the immunological processes driving rejection and highlight the potential of AqH proteomics for clinical application.

AqH has emerged as an important diagnostic medium for various ocular conditions. As a biofluid that is in constant contact with the cornea, AqH serves as a unique source of biomarkers that can reflect real-time changes in the ocular microenvironment. Recent proteomic and cytokine profiling techniques have positioned AqH as a rich source of potential biomarkers for neurodegenerative and inflammatory ocular diseases.[15,17,18,36] The limited sample volume (50-150 μL) and low protein concentration (0.1-0.6 μg/mL) necessitate highly sensitive detection methods. Additionally, the wide dynamic range of AqH poses further technical challenges in biomarker discovery.[37] However, current advancements in mass spectrometry and affinity-based techniques have improved our ability to analyze AqH samples, even with these limitations, making AqH proteomics a feasible and promising diagnostic tool for clinical application.

Previous studies investigating biomarkers for corneal allograft rejection have primarily relied on tissue biopsies. Di Zazzo *et al.* reported that decreased Foxp3 in Tregs expression increases rejection risk.[20] Elevated levels of VEGF-A, VEGF-C, and VEGF-D in corneal grafts have been also shown to significantly heighten rejection risk.[22] Additionally, increased immune cell density in the sub-basal and endothelial layers of the cornea proposed as an indicator of an active rejection process.[20] In parallel, blood-based biomarkers have also been investigated. Yoon *et al.* demonstrated that elevated levels of CD8+IFNγ+ T cells in peripheral blood are linked to an increased risk of corneal xenograft rejection.[18] The presence of circulating donor-specific antibodies, particularly those directed against donor class I HLA, has been associated with immune-mediated graft failure.[38]

However, these sources of biomarkers involve invasive procedures and may not be suitable for detecting early-stage rejection. Tissue biopsies, in particular, are impractical during the early phases of rejection, as biopsies themselves may induce or exacerbate rejection due to the invasive nature of the procedure. This limitation emphasizes the significance of liquid biopsy techniques like AqH analysis.

The present study highlights the potential of AqH as a minimally-invasive and more practical alternative for early detection of corneal graft rejection. Unlike tissue or blood samples, AqH, being in direct contact with the cornea, serves as an ideal candidate for liquid biopsy to detect molecular changes in the corneal environment during graft acceptance, immune surveillance, and rejection. By employing proteomic analysis of AqH, our study circumvents the challenges of tissue biopsies, offering a minimally invasive method to monitor graft health (Figure 12A). This novel approach could address the limitations of conventional methods, such as slit-lamp microscopy, which often detect rejection only after clinical signs become evident. Consequently, our data show that proteins involved in immune activation and oxidative stress pathways are consistently upregulated in AqH prior to overt clinical signs of rejection. This demonstrates that AqH can serve as a reliable and early indicator of graft rejection, allowing for prompt therapeutic intervention.

The proteomic analysis of murine and human AqH revealed significant upregulation of BLVRB in both rejected grafts and transitional allografts, suggesting its active involvement during the rejection process. BLVRB’s primary function—the NADPH-dependent reduction of biliverdin to bilirubin—plays a crucial role in providing antioxidant defense by regulating cellular redox states.[39] Oxidative stress is a key driver of inflammation and tissue damage, and BLVRB's role in mitigating these effects is central to its function in immune regulation. Studies have demonstrated BLVRB's ability to modulate immune responses, particularly through the PI3K-Akt-IL-10 signaling axis, which downregulates pro-inflammatory cytokine production, further supporting its anti-inflammatory role.[40] BLVRB also helps suppress pro-inflammatory signaling by inhibiting TLR4 expression, regulating macrophage activity.[40] This aligns with our findings, where BLVRB was consistently upregulated in the AqH of both the Allo-I and Allo-R groups, suggesting that BLVRB contributes to immune modulation during both transitional and full rejection phases.

Interestingly, to our knowledge, this study may be the first to report the expression of biliverdin reductase in AqH during graft rejection. Previous one study has identified BLVRB in zebrafish retinal tissues, where its expression is induced by environmental stressors such as light-induced

oxidative damage, functioning in heme catabolism and redox balance.[41] In the context of corneal allograft rejection, the upregulation of BLVRB in AqH during rejection suggests that its protective mechanisms are activated to counter oxidative stress and immune activation. The fact that BLVRB is consistently upregulated in both murine and human samples during rejection supports the hypothesis that its function in managing oxidative stress and protecting ocular tissues from immune-mediated damage is essential for graft survival.

The biliverdin-bilirubin pathway, mediated by BLVRB, has demonstrated protective effects in transplantation models.[42-44] Yamashita *et al.* have shown that biliverdin administration induces tolerance in cardiac allografts by inhibiting T cell signaling, particularly by reducing activation of nuclear factor of activated T cells (NFAT) and nuclear factor kappaB, and suppressing interferon-gamma production.[44] Another study reported that biliverdin administration reduced transplantation-induced injuries in small bowel grafts, improving recipient survival by attenuating inflammation.[45] In the case of corneal transplantation, the upregulation of BLVRB observed in our proteomic analysis of rejected grafts further suggests that this enzyme is a part of the body's intrinsic defense mechanism against immune-mediated graft rejection.

Given these findings, therapeutic strategies targeting BLVRB could be explored to modulate its protective effects and reduce the incidence of corneal allograft rejection. Administering biliverdin or modulating BLVRB activity might help in reducing oxidative stress and controlling immune responses, potentially improving outcomes for corneal allografts and other organ transplants. The consistent upregulation of BLVRB across murine and human AqH samples highlights its importance during graft rejection. Its dual role in redox regulation and immune modulation makes it a promising candidate for further research, both as a biomarker for early detection and as a potential therapeutic target in corneal allograft rejection.

Similarly, GPX1 (glutathione peroxidase 1), another key antioxidant enzyme, was upregulated, reflecting the ongoing oxidative stress in the AqH during rejection. Although GPX1 was detected in the murine AqH during both transitional and rejection phases, our study did not detect GPX1 in human AqH; instead, a related GPX isoform was found (Figure 11 and 13). While there is limited evidence of GPX1's direct involvement in acute rejection and chronic allograft transplantation, previous studies in kidney transplantation suggest that the GPX system plays a critical role in maintaining antioxidant defenses during the post-transplant period.[46,47] Specifically, these studies highlighted that successful kidney transplantation can rapidly restore GPX activity, and monitoring

GPX activity could potentially serve as an indicator of graft function early after transplantation.[46]

GPX1 is a well-known antioxidant enzyme that protects cells from oxidative damage by neutralizing reactive oxygen species. GPX1-deficient models have demonstrated heightened oxidative damage and increased vulnerability to tissue injury during conditions such as ischemia-reperfusion injury, a common challenge in transplantation.[48] This suggests that GPX1 may play a protective role in transplanted corneal tissues, particularly during the early postoperative period when oxidative stress is elevated due to graft reoxygenation.

Given GPX1's established role in reducing oxidative stress and modulating immune responses, its upregulation in the murine model highlights a potential therapeutic target. Enhancing GPX activity, whether through upregulation of GPX1 or related GPX isoforms, may help mitigate oxidative stress and improve graft survival. Antioxidant therapies that target the GPX pathways, such as selenium supplementation (a necessary cofactor for GPX1 activity), could be explored as a strategy to reduce corneal allograft rejection rates. Further research into the specific GPX isoforms involved in human corneal graft rejection may provide additional insights into potential interventions to optimize graft outcomes.

Cystatin B (CSTB), a cysteine protease inhibitor, emerged as a significantly upregulated protein in both murine and human AqH during the transitional and rejection phases of corneal allograft rejection (Figures 11 and 13). CSTB plays a critical role in regulating inflammation, protecting cells from protease-mediated damage, and controlling oxidative stress, all of which are key factors during graft rejection.[49-51] Previous studies have shown that CSTB-deficient models exhibit enhanced inflammation with an increased release of nitric oxide from immune cells, suggesting CSTB normally acts to suppress excessive immune responses.[50] Additionally, Cystatin B-deficient mice display increased sensitivity to sepsis and elevated production of pro-inflammatory cytokines like IL-1β and IL-18, highlighting its role in mitigating inflammatory pathways.[51]

CSTB's ability to protect cells from oxidative stress is particularly important in the immune-privileged environment of the eye, where oxidative stress can exacerbate tissue damage and drive graft rejection. Recent studies demonstrate that CSTB helps maintain cellular homeostasis under oxidative stress by inhibiting cathepsins and preventing uncontrolled proteolytic activity.[52] CSTB also is involved in controlling cell proliferation and differentiation, synaptic functions and protection against oxidative stress, likely through regulation of mitochondrial function. This protective effect could be vital in prolonging graft survival by minimizing oxidative damage to corneal cells,

especially during heightened immune responses seen during graft rejection.

Although direct evidence linking CSTB to corneal transplantation outcomes is limited, its biological functions suggest CSTB plays a key role in regulating immune activation and protecting corneal tissues from inflammatory damage during the rejection process. In our study, CSTB was consistently upregulated in both murine and human AqH samples during the transitional and rejection phases, indicating that its role in immune regulation and tissue protection is likely activated during the rejection process. CSTB's increased expression in the AqH implies that it may help limit protease-mediated tissue degradation, a critical factor in graft survival.

While prior research on CSTB has not directly addressed its role in transplantation, our findings suggest that its biological functions, particularly its ability to regulate inflammation and oxidative stress, could influence transplant outcomes. However, further investigation is required to confirm the specific role of CSTB in corneal transplantation and its potential as a therapeutic target for reducing allograft rejection rates.

The corneal transcriptome data from murine models (Supplementary Figures 2 and 3) support our findings. The transcriptomic analysis revealed significant upregulation of immune-related genes, particularly in the Allo-I and Allo-R corneas, which corresponded with the proteomic changes observed in AqH. Additionally, the Allo-A cornea's unique transcriptomic profile suggests that graft acceptance involves active immune regulation, consistent with prior studies indicating that accepted allografts maintain immune tolerance through active modulation (Supplementary Figure 2).[53,54] Interestingly, a PPI network analysis of DEGs from the Allo-I and Allo-R corneas highlighted several key biological processes, particularly those related to immune system responses (Supplementary Figure 3). In this cluster, genes such as Ppp3r1, Rho, and Sod1 are more highly expressed in the Allo-I corneas compared to the Allo-R. Especially, Ppp3r1, a regulatory subunit of calcineurin, plays a critical role in T-cell activation through the NFAT pathway and Nurr77 signaling, both of which are pivotal in driving immune responses during graft rejection.[55-57]

Despite the valuable insights gained from this study, limitations must be acknowledged. One of the main limitations is the inability to sample AqH from patients with accepted or intermediate-stage grafts. This limitation restricts our ability to fully capture the proteomic and immune dynamics during the critical transition from immune tolerance to rejection in human corneal transplants. However, the overlap observed between murine and human proteomic data offers a strong foundation for the potential clinical application of AqH biomarkers. While murine models provide

controlled insight into immune processes, further studies are needed to validate these biomarkers in diverse human populations, particularly in the early stages of rejection or immune tolerance.

In addition, although this study demonstrates the utility of AqH proteomics, there remain practical challenges in collecting AqH samples from patients in routine clinical settings, especially before clinical signs of rejection appear. This raises the need for improved, minimally-invasive sampling techniques to monitor corneal graft health more frequently. Despite these limitations, our findings contribute to the growing body of evidence that immune-related proteins in AqH play a central role in graft rejection, suggesting that AqH analysis could serve as a valuable tool for the early detection and prediction of corneal allograft rejection in clinical practice.

# V. CONCLUSION

This study provides novel insights into the molecular mechanisms underlying corneal allograft rejection by identifying key proteins in the AqH that may serve as biomarkers for early detection and intervention. Due to the clinical challenge of distinguishing early signs of rejection, we aimed to identify biomarkers that represent the molecular changes occurring before clinical symptoms appear. Through the use of AqH liquid biopsy, we were able to capture these early molecular alterations and propose BLVRB, GPX1, and CSTB as potential biomarkers for corneal allograft rejection.

BLVRB, as a key enzyme involved in redox regulation, emerged as a central player in managing oxidative stress during graft rejection. Its upregulation across both murine and human samples highlights its importance in mitigating tissue damage during immune activation. Similarly, GPX1, another potent antioxidant enzyme, was upregulated, reflecting the ongoing efforts to control oxidative damage. CSTB, a cysteine protease inhibitor, further contributed to immune regulation by preventing excessive proteolytic activity and tissue degradation.

The identification of these proteins as biomarkers not only provides insight into the rejection process but also offers a minimally invasive diagnostic tool using AqH proteomics, which could allow for early detection and timely therapeutic intervention. This approach circumvents the limitations of conventional clinical methods, which often detect rejection only after significant tissue damage has occurred.

While these findings provide a solid foundation for the use of AqH proteomics in clinical practice, further studies are necessary to validate these biomarkers in larger and more diverse patient populations. Additionally, exploring therapeutic strategies that target these key proteins could offer new approaches to improving graft survival rates, particularly through antioxidant therapies or immune modulation.

In conclusion, by identifying BLVRB, GPX1, and CSTB as critical proteins involved in the rejection process, this study highlights the potential of AqH liquid biopsy for the early detection of corneal allograft rejection. These findings could significantly enhance the clinical management of corneal allograft recipients, improving both graft survival and patient outcomes.

# REFERENCES

1. Armitage WJ, Goodchild C, Griffin MD, Gunn DJ, Hjortdal J, Lohan P, et al. High-risk Corneal Transplantation: Recent Developments and Future Possibilities. Transplantation 2019;103:2468-78.
2. Liu S, Wong YL, Walkden A. Current Perspectives on Corneal Transplantation. Clin Ophthalmol 2022;16:631-46.
3. Hori J, Yamaguchi T, Keino H, Hamrah P, Maruyama K. Immune privilege in corneal transplantation. Prog Retin Eye Res 2019;72:100758.
4. Wong YL, Liu S, Walkden A. Current Perspectives on Corneal Transplantation (Part 2). Clin Ophthalmol 2022;16:647-59.
5. Yin J. Advances in corneal graft rejection. Curr Opin Ophthalmol 2021;32:331-7.
6. Azevedo Magalhaes O, Shalaby Bardan A, Zarei-Ghanavati M, Liu C. Literature review and suggested protocol for prevention and treatment of corneal graft rejection. Eye (Lond) 2020;34:442-50.
7. Alio JL, Montesel A, El Sayyad F, Barraquer RI, Arnalich-Montiel F, Alio Del Barrio JL. Corneal graft failure: an update. Br J Ophthalmol 2021;105:1049-58.
8. Gain P, Jullienne R, He Z, Aldossary M, Acquart S, Cognasse F, et al. Global Survey of Corneal Transplantation and Eye Banking. JAMA Ophthalmol 2016;134:167-73.
9. Musa M, Zeppieri M, Enaholo ES, Chukwuyem E, Salati C. An Overview of Corneal Transplantation in the Past Decade. Clin Pract 2023;13:264-79.
10. Shin KY, Lim DH, Han K, Chung TY. Higher incidence of penetrating keratoplasty having effects on repeated keratoplasty in South Korea: A nationwide population-based study. PLoS One 2020;15:e0235233.
11. Mandal S, Maharana PK, Kaweri L, Asif MI, Nagpal R, Sharma N. Management and prevention of corneal graft rejection. Indian J Ophthalmol 2023;71:3149-59.
12. Gurnani B, Czyz CN, Mahabadi N, Havens SJ. Corneal Graft Rejection. StatPearls. Treasure Island (FL); 2024.
13. Tabbara KF. Pharmacologic strategies in the prevention and treatment of corneal transplant rejection. Int Ophthalmol 2008;28:223-32.
14. Berry JL, Pike S, Shah R, Reid MW, Peng CC, Wang Y, et al. Aqueous Humor Liquid Biopsy as a Companion Diagnostic for Retinoblastoma: Implications for Diagnosis,

Prognosis, and Therapeutic Options: Five Years of Progress. Am J Ophthalmol 2024;263:188-205.

15. Moon CE, Kim CH, Jung JH, Cho YJ, Choi KY, Han K, et al. Integrated Analysis of Transcriptome and Proteome of the Human Cornea and Aqueous Humor Reveal Novel Biomarkers for Corneal Endothelial Cell Dysfunction. Int J Mol Sci 2023;24.
16. Zubair H, Azim S, Maluf DG, Mas VR, Martins PN. Contribution of Proteomics in Transplantation: Identification of Injury and Rejection Markers. Transplantation 2023;107:2143-54.
17. Oh JW, Yoon CH, Ryu JS, Kim KP, Kim MK. Proteomics Analysis of Aqueous Humor and Rejected Graft in Pig-to-Non-Human Primate Corneal Xenotransplantation. Front Immunol 2022;13:859929.
18. Yoon CH, Choi SH, Lee HJ, Kang HJ, Kim MK. Predictive biomarkers for graft rejection in pig-to-non-human primate corneal xenotransplantation. Xenotransplantation 2019;26:e12515.
19. Boisgerault F, Liu Y, Anosova N, Ehrlich E, Dana MR, Benichou G. Role of CD4+ and CD8+ T cells in allorecognition: lessons from corneal transplantation. J Immunol 2001;167:1891-9.
20. Di Zazzo A, Lee SM, Sung J, Niutta M, Coassin M, Mashaghi A, et al. Variable Responses to Corneal Grafts: Insights from Immunology and Systems Biology. J Clin Med 2020;9.
21. Eleiwa T, Elsawy A, Ozcan E, Chase C, Feuer W, Yoo SH, et al. Prediction of corneal graft rejection using central endothelium/Descemet's membrane complex thickness in high-risk corneal transplants. Sci Rep 2021;11:14542.
22. Sakowska J, Glasner P, Zielinski M, Trzonkowski P, Glasner L. Corneal Allografts: Factors for and against Acceptance. J Immunol Res 2021;2021:5372090.
23. Blanco T, Singh RB, Nakagawa H, Taketani Y, Dohlman TH, Chen Y, et al. Conventional type I migratory CD103(+) dendritic cells are required for corneal allograft survival. Mucosal Immunol 2023;16:711-26.
24. Yin XT, Tajfirouz DA, Stuart PM. Murine corneal transplantation: a model to study the most common form of solid organ transplantation. J Vis Exp 2014; doi:10.3791/51830.e51830.
25. Zhu J, Inomata T, Nakamura M, Fujimoto K, Akasaki Y, Fujio K, et al. Anti-CD80/86

antibodies inhibit inflammatory reaction and improve graft survival in a high-risk murine corneal transplantation rejection model. Sci Rep 2022;12:4853.

26. Chen P, Park KH, Zhang L, Lucas AR, Chandler HL, Zhu H. Mouse Corneal Transplantation. Methods Mol Biol 2023;2597:19-24.
27. Inomata T, Mashaghi A, Di Zazzo A, Dana R. Ocular surgical models for immune and angiogenic responses. J Biol Methods 2015;2.
28. Ko MK, Yelenskiy A, Gonzalez JM, Jr., Tan JC. Feedback-controlled constant-pressure anterior chamber perfusion in live mice. Mol Vis 2014;20:163-70.
29. Tan JC, Ko MK, Woo JI, Lu KL, Kelber JA. Aqueous humor TGFbeta and fibrillin-1 in Tsk mice reveal clues to POAG pathogenesis. Sci Rep 2024;14:3517.
30. Kim D, Langmead B, Salzberg SL. HISAT: a fast spliced aligner with low memory requirements. Nat Methods 2015;12:357-60.
31. Pertea M, Pertea GM, Antonescu CM, Chang TC, Mendell JT, Salzberg SL. StringTie enables improved reconstruction of a transcriptome from RNA-seq reads. Nat Biotechnol 2015;33:290-5.
32. Pertea M, Kim D, Pertea GM, Leek JT, Salzberg SL. Transcript-level expression analysis of RNA-seq experiments with HISAT, StringTie and Ballgown. Nat Protoc 2016;11:1650-67.
33. Robinson MD, McCarthy DJ, Smyth GK. edgeR: a Bioconductor package for differential expression analysis of digital gene expression data. Bioinformatics 2010;26:139-40.
34. Elias C, Chen C, Cherukuri A. Regulatory B Cells in Solid Organ Transplantation: From Immune Monitoring to Immunotherapy. Transplantation 2024;108:1080-9.
35. Shipkova M, Wieland E. Editorial: Immune monitoring in solid organ transplantation. Clin Biochem 2016;49:317-9.
36. Lee SH, Jung JH, Park TK, Moon CE, Han K, Lee J, et al. Proteome alterations in the aqueous humor reflect structural and functional phenotypes in patients with advanced normal-tension glaucoma. Sci Rep 2022;12:1221.
37. Beutgen VM, Graumann J. Advances in aqueous humor proteomics for biomarker discovery and disease mechanisms exploration: a spotlight on primary open angle glaucoma. Front Mol Neurosci 2024;17:1397461.
38. Major J, Foroncewicz B, Szaflik JP, Mucha K. Immunology and Donor-Specific Antibodies

in Corneal Transplantation. Arch Immunol Ther Exp (Warsz) 2021;69:32.

39. Duff MR, Redzic JS, Ryan LP, Paukovich N, Zhao R, Nix JC, et al. Structure, dynamics and function of the evolutionarily changing biliverdin reductase B family. J Biochem 2020;168:191-202.
40. Wegiel B, Otterbein LE. Go green: the anti-inflammatory effects of biliverdin reductase. Front Pharmacol 2012;3:47.
41. Connor B, Titialii-Torres K, Rockenhaus AE, Passamonte S, Morris AC, Lee YS. Biliverdin regulates NR2E3 and zebrafish retinal photoreceptor development. Sci Rep 2022;12:7310.
42. Ollinger R, Wang H, Yamashita K, Wegiel B, Thomas M, Margreiter R, et al. Therapeutic applications of bilirubin and biliverdin in transplantation. Antioxid Redox Signal 2007;9:2175-85.
43. Nakao A, Neto JS, Kanno S, Stolz DB, Kimizuka K, Liu F, et al. Protection against ischemia/reperfusion injury in cardiac and renal transplantation with carbon monoxide, biliverdin and both. Am J Transplant 2005;5:282-91.
44. Yamashita K, McDaid J, Ollinger R, Tsui TY, Berberat PO, Usheva A, et al. Biliverdin, a natural product of heme catabolism, induces tolerance to cardiac allografts. FASEB J 2004;18:765-7.
45. Nakao A, Otterbein LE, Overhaus M, Sarady JK, Tsung A, Kimizuka K, et al. Biliverdin protects the functional integrity of a transplanted syngeneic small bowel. Gastroenterology 2004;127:595-606.
46. Zachara BA, Wlodarczyk Z, Andruszkiewicz J, Gromadzinska J, Wasowicz W. Glutathione and glutathione peroxidase activities in blood of patients in early stages following kidney transplantation. Ren Fail 2005;27:751-5.
47. Dutkiewicz G, Binczak-Kuleta A, Pawlik A, Safranow K, Wisniewska M, Ciechanowicz A, et al. Lack of association of C599T polymorphism in the glutathione peroxidase (GPX1) gene with delayed graft function, acute kidney graft rejection and chronic allograft nephropathy. Ann Transplant 2010;15:30-4.
48. Pei J, Pan X, Wei G, Hua Y. Research progress of glutathione peroxidase family (GPX) in redoxidation. Front Pharmacol 2023;14:1147414.
49. Contini C, Serrao S, Manconi B, Olianas A, Iavarone F, Guadalupi G, et al. Characterization of Cystatin B Interactome in Saliva from Healthy Elderly and Alzheimer's Disease Patients.

Life (Basel) 2023;13.

50. Okuneva O, Li Z, Korber I, Tegelberg S, Joensuu T, Tian L, et al. Brain inflammation is accompanied by peripheral inflammation in Cstb (-/-) mice, a model for progressive myoclonus epilepsy. J Neuroinflammation 2016;13:298.
51. Kopitar-Jerala N. The Role of Stefin B in Neuro-inflammation. Front Cell Neurosci 2015;9:458.
52. Singh S, Hamalainen RH. The Roles of Cystatin B in the Brain and Pathophysiological Mechanisms of Progressive Myoclonic Epilepsy Type 1. Cells 2024;13.
53. Robinson KA, Orent W, Madsen JC, Benichou G. Maintaining T cell tolerance of alloantigens: Lessons from animal studies. Am J Transplant 2018;18:1843-56.
54. VanBuskirk AM, Burlingham WJ, Jankowska-Gan E, Chin T, Kusaka S, Geissler F, et al. Human allograft acceptance is associated with immune regulation. J Clin Invest 2000;106:145-55.
55. Lith SC, van Os BW, Seijkens TTP, de Vries CJM. 'Nur'turing tumor T cell tolerance and exhaustion: novel function for Nuclear Receptor Nur77 in immunity. Eur J Immunol 2020;50:1643-52.
56. Spivey TL, Uccellini L, Ascierto ML, Zoppoli G, De Giorgi V, Delogu LG, et al. Gene expression profiling in acute allograft rejection: challenging the immunologic constant of rejection hypothesis. J Transl Med 2011;9:174.
57. Mencarelli A, Vacca M, Khameneh HJ, Acerbi E, Tay A, Zolezzi F, et al. Calcineurin B in CD4(+) T Cells Prevents Autoimmune Colitis by Negatively Regulating the JAK/STAT Pathway. Front Immunol 2018;9:261.

# APPENDICES

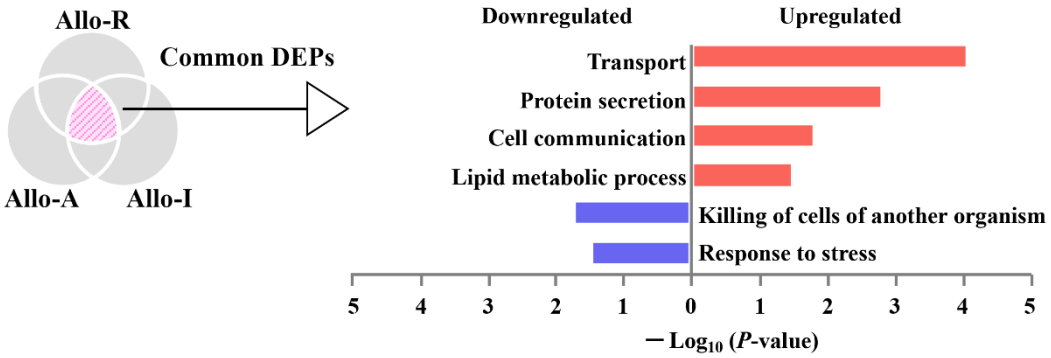


**Supplementary Figure 1.** Venn Diagrams Illustrating the Common Differentially Expressed Proteins (DEPs) among the Allogeneic Keratoplasty Groups (Allo-A, Allo-I, and Allo-R). Gene Ontology biological process enriched by common DEPs in the allogeneic KP groups.

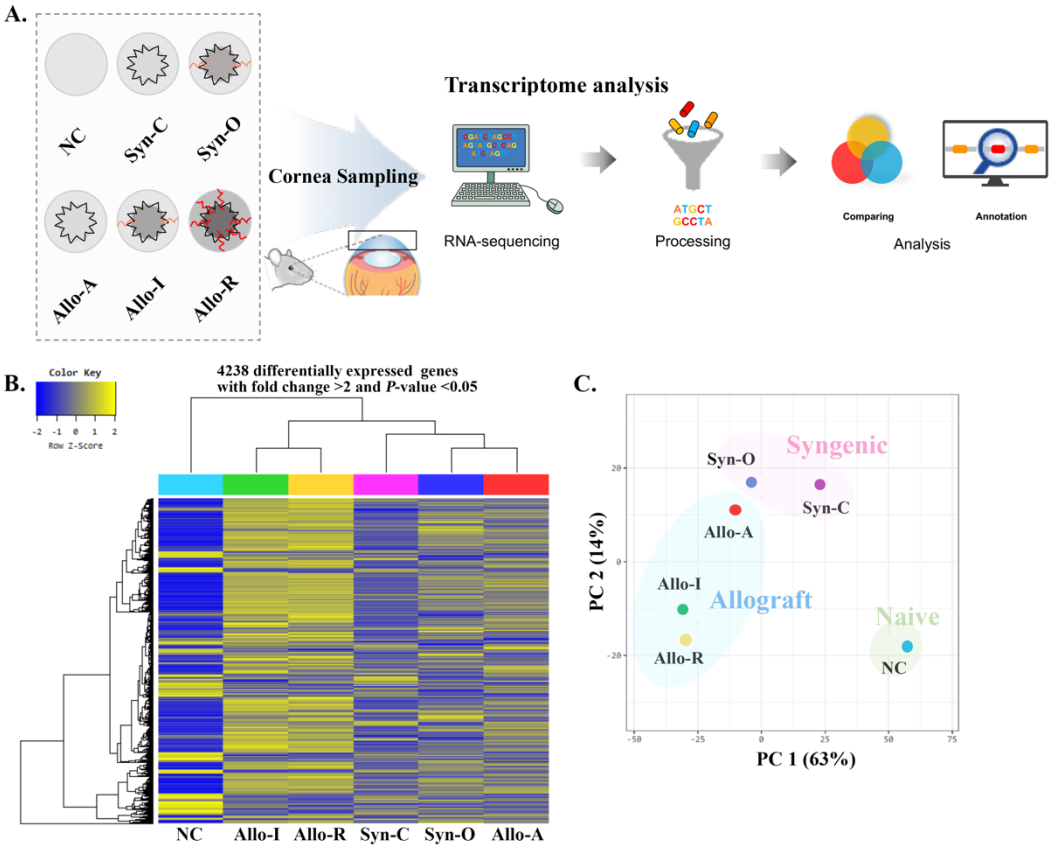


**Supplementary Figure 2.** Transcriptome Analysis of Corneal Tissues in Murine Keratoplasty Models

**A.** Experimental workflow depicting the corneal sampling and RNA-sequencing process for transcriptome analysis across six experimental groups: naïve control (NC), syngeneic keratoplasty (KP)-clear (Syn-C), syngeneic KP-opaque (Syn-O), allogeneic KP-accepted (Allo-A), allogeneic KP-intermediate (Allo-I), and allogeneic KP-rejected (Allo-R).

**B.** Heatmap showing the hierarchical clustering of 4,238 differentially expressed genes (DEGs) with a fold change >2 and P-value < 0.05. Each row represents a gene, and each column represents an experimental group, with color indicating the Z-score for gene expression levels.

**C.** Principal Component Analysis plot of the transcriptomic profiles from corneal tissues.

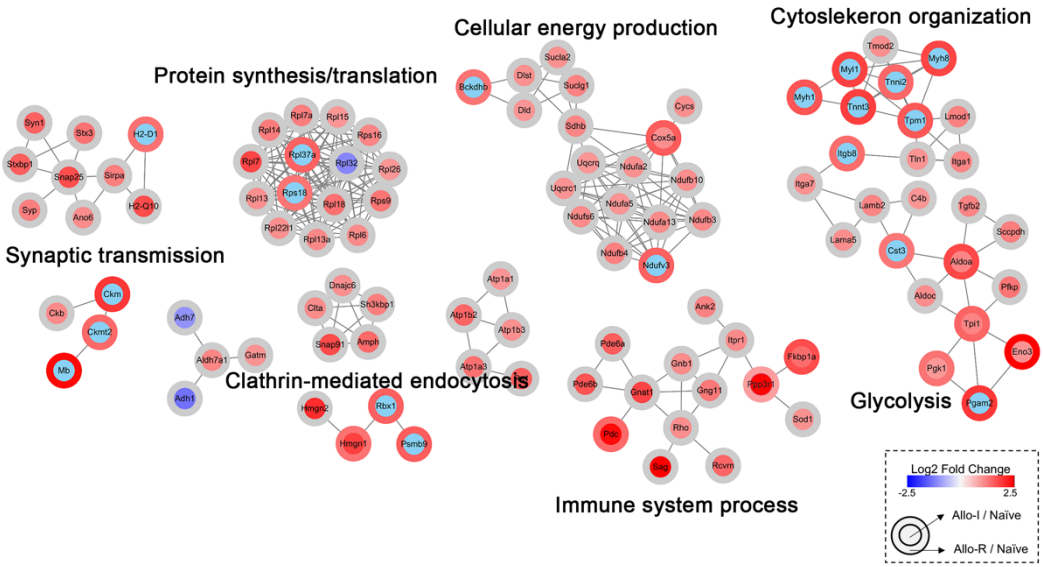


**Supplementary Figure 3.** Protein-Protein Interaction Network of Differentially Expressed Genes In the Corneal Allograft During Rejection

This figure presents the protein-protein Interaction network of differentially expressed genes (DEGs) in the corneal tissue of the allogeneic keratoplasty (KP)-intermediate (Allo-I) and allogeneic KP-rejected (Allo-R) groups compared to the Naïve control group. Red nodes indicate upregulated DEGs, and blue nodes indicate downregulated DEGs.

Abstract in Korean

# 방수 액체 생검을 활용한 동종 각막 이식 거부 반응의 기전 및 주요 인자 연구

**목적:** 각막 이식에서 이식편 거부반응은 특히 고위험 환자에서 여전히 중요한 문제로 남아 있다. 임상양상이 발현하기 이전에 거부반응을 조기에 발견하는 것은 이식편의 생존율을 높이기 위해서 매우 중요하다. 본 연구는 방수를 이용한 액체 생검을 통해 동종 각막 이식에서 거부반응의 주요 기전과 핵심 인자를 규명하고자 하였다.
**방법:** 동종 이식편의 거부반응 면역 과정을 모사하기 위해 동종 이종 각막이식 마우스 모델을 사용하였다. 수용된 이식편, 거부반응으로 진행 중인 이식편, 그리고 완전히 거부된 이식편 등으로 그룹을 나누어 방수와 각막 조직을 채취한 후 포괄적인 단백체 및 전사체 분석을 실시하였다. 뿐만 아니라, 마우스 모델에서 도출한 마커물질을 검증하기 위해 각막이식 후 거부반응이 발생한 환자와 건강한 대조군에서 방수 샘플을 수집하여 분석하였다.
**결과:** 마우스 모델에서 단백체 및 전사체 분석을 통해 이식편 거부반응의 단계별로 상이한 분자생물학적 프로파일이 나타났다. 특히, 빌리베르딘 환원효소 B(BLVRB), 글루타티온 퍼옥시다제 1(GPX1), 시스타틴 B(CSTB)가 동물 모델과 인간 방수 모두에서 거부반응이 진행 중일 때와 거부된 상태에서 유의하게 발현이 증가하였다. 이들 단백질은 산화 스트레스 반응과 면역 조절에 관여하며, 임상 증상이 나타나기 전 이식편의 거부반응을 예측할 수 있는 초기 바이오마커로서 가능성을 보여주었다.
**결론:** 본 연구는 방수를 이용한 비침습적 액체 생검이 각막 동종이식편의 거부반응과 관련된 분자적 변화를 조기에 감지하는데 유용함을 입증하였다. 뿐만 아니라, BLVRB, GPX1, CSTB 를 주요 방수 바이오마커로 규명함으로써, 조기 진단을 통하여 빠른 치료를 함으로써 이식편의 생존율을 향상시킬 수 있는 새로운 접근 방안을 제시하였다.

---

**핵심되는 말** : 각막 이식, 방수, 바이오마커, 단백체, 이식편 거부반응, 액체 생검, 빌리베르딘 환원효소 B, 글루타티온 퍼옥시다제 1, 시스타틴 B.

# PUBLICATION LIST

1. Neutralization of ocular surface TNF-α reduces ocular surface and lacrimal gland inflammation induced by in vivo dry eye.

**Ji YW**, Byun YJ, Choi W, Jeong E, Kim JS, Noh H, Kim ES, Song YJ, Park SK, and Lee HK. **(Co-first author)**

*Invest Ophthalmol Vis Sci.* 2013 Nov 15;54(12):7557-66

2. Activation of HIF-1α (hypoxia inducible factor-1α) prevents dry eye-induced acinar cell death in the lacrimal gland.

Seo Y, **Ji YW**, Lee SM, Shim J, Noh H, Yeo A, Park C, Park MS, Chang EJ, and Lee HK. **(Co-first author)**

*Cell Death Dis.* 2014 Jun 26;5:e1309.

3. Dry eye-induced CCR7+CD11b+ cell lymph node homing is induced by COX-2 activities.

**Ji YW**, Seo Y, Choi W, Yeo A, Noh H, Kim EK, and Lee HK. **(Co-first author)**

*Invest Ophthalmol Vis Sci.* 2014 Sep 25;55(10):6829-38

4. Lacrimal gland-derived IL-22 regulates IL-17-mediated ocular mucosal inflammation.

**Ji YW**, Mittal SK, Hwang HS, Chang EJ, Lee JH, Seo Y, Yeo A, Noh H, Lee HS, Chauhan SK, Lee HK. **(First author)**

*Mucosal Immunol.* 2017 Sep;10(5):1202-121

5. Proteomic analysis of human lacrimal and tear fluid in dry eye disease.

Jung JH, **Ji YW**, Hwang HS, Oh JW, Kim HC, Lee HK, Kim KP.

*Sci Rep.* 2017 Oct 17;7(1):13363.

6. p-Coumaroyl anthocyanin mixture isolated from tuber epidermis of solanum tuberosum attenuates reactive oxygen species and pro-inflammatory mediators

by suppressing NF-κB and STAT1/3 signaling in LPS-induced RAW264.7 macrophages.

Lee HH, Lee SG, Shin JS, Lee HY, Yoon K, **Ji YW**, Jang DS, Lee KT.

*Biol Pharm Bull.* 2017;40(11):1894-1902.

7. Corneal lymphangiogenesis facilitates ocular surface inflammation and cell trafficking in dry eye disease.

**Ji YW**, Lee JL, Kang HG, Gu N, Byun H, Yeo A, Noh H, Kim S, Choi EY, Song JS, Lee HK. **(Co-first author)**

*Ocul Surf.* 2018 Jul;16(3):306-313.

8. Comparison of ocular surface mucin expression after topical ophthalmic drug administration in dry eye-induced mouse model.

Moon I, Kang HG, Yeo A, Noh H, Kim HC, Song JS, **Ji YW**, Lee HK. **(Co-corresponding author)**

*J Ocul Pharmacol Ther.* 2018 Nov;34(9):612-620.

9. Downregulation of IL-7 and IL-7R reduces membrane-type matrix metalloproteinase 14 in granular corneal dystrophy type 2 keratocyte.

Kim SY, Yeo A, Noh H, **Ji YW**, Song JS, Kim HC, Kim LK, Lee HK.

*Invest Ophthalmol Vis Sci.* 2018 Nov 1;59(13):5693-5703.

10. Changes in human tear proteome following topical treatment of dry eye disease: Cyclosporine A versus diquafosol tetrasodium.

**Ji YW**, Kim HM, Ryu SY, Oh JW, Yeo A, Choi CY, Kim MJ, Song JS, Kim HS, Seo KY, Kim KP, Lee HK. **(Co-first author)**

*Invest Ophthalmol Vis Sci.* 2019 Dec 2;60(15):5035-5044.

11. Alterations of aqueous humor Aβ levels in Aβ-infused and transgenic mouse models of Alzheimer disease.

Kwak DE, Ko T, Koh HS, **Ji YW**, Shin J, Kim K, Kim HY, Lee HK, Kim Y.
*PLoS One.* 2020 Jan 10;15(1):e0227618.

12. HIF1α-mediated TRAIL expression regulates lacrimal gland inflammation in dry eye disease.

**Ji YW**, Lee JH, Choi EY, Kang HG, Seo KY, Song JS, Kim HC, Lee HK. **(First author)**
*Invest Ophthalmol Vis Sci.* 2020 Jan 23;61(1):3.

13. Matrix metalloproteinase 9-activatable peptide-conjugated hydrogel-based fluorogenic intraocular-lens sensor.

Shin MK, **Ji YW**, Moon CE, Lee H, Kang B, Jinn WS, Ki J, Mun B, Kim MH, Lee HK, Haam S. **(Co-first author)**
*Biosens Bioelectron.* 2020 Aug 15;162:112254.

14. The correction of conjunctivochalasis using high-frequency radiowave electrosurgery improves dry eye disease.

**Ji YW**, Seong H, Lee S, Alotaibi MH, Kim TI, Lee HK, Seo KY. **(First author)**
*Sci Rep.* 2021 Jan 28;11(1):2551.

15. Compound heterozygous mutations in TGFBI cause a severe phenotype of granular corneal dystrophy type 2

Jun I, **Ji YW**, Choi SI, Lee BR, Min JS, Kim EK. **(Co-first author)**
*Sci Rep.* 2021 Mar 26;11(1):6986.

16. The dopaminergic neuronal system regulates the inflammatory status of mouse lacrimal glands in dry eye disease.

**Ji YW**, Kang HG, Song JS, Jun JW, Han K, Kim TI, Seo KY, Lee HK. **(Co-first author)**
*Invest Ophthalmol Vis Sci.* 2021 Apr 1;62(4):14.

17. Proteome alterations in the aqueous humor reflect structural and functional phenotypes in patients with advanced normal-tension glaucoma.

Lee SH, Jung JH, Park TK, Moon CE, Han K, Lee J, Lee HK, **Ji YW**, Kim CY. **(Co-corresponding author)**

*Sci Rep.* 2022 Jan 24;12(1):1221.

18. Long-term follow-up of corneal endothelial cell changes after iris-fixated phakic intraocular lens explantation.

Kim TY, Moon IH, Park SE, **Ji YW**, Lee HK.

*Cornea.* 2023 Feb 1;42(2):150-155.

19. Evaluation of meibum lipid composition according to tear interferometric patterns: Meibum composition according to interferometric patterns.

Jun I, Kim S, Kim H, Kim SW, **Ji YW**, Kim KP, Lee TG, Seo KY.

*Am J Ophthalmol.* 2022 Aug;240:37-50.

20. Tissue extracellular matrix hydrogels as alternatives to Matrigel for culturing gastrointestinal organoids.

Kim S, Min S, Choi YS, Jo SH, Jung JH, Han K, Kim J, An S, **Ji YW**, Kim YG, Cho SW.

*Nat Commun.* 2022 Mar 30;13(1):1692.

21. Correlation between salivary microbiome of parotid glands and clinical features in primary Sjögren's syndrome and non-Sjögren's sicca subjects.

Kim D, Jeong YJ, Lee Y, Choi J, Park YM, Kwon OC, **Ji YW**, Ahn SJ, Lee HK, Park MC, Lim JY.

*Front Immunol.* 2022 May 4;13:874285.

22. De novo L509P mutation of the TGFBI gene associated with slit-lamp findings of lattice corneal dystrophy type IIIA.

**Ji YW**, Ahn H, Shin KJ, Kim TI, Seo KY, Stulting RD, Kim EK. **(Co-first author)**

*J Clin Med.* 2022 May 28;11(11):3055.

23. Real-time and label-free biosensing using moiré pattern generated by bioresponsive hydrogel.

Kim S, Kim G, **Ji YW**, Moon CE, Jung Y, Lee HK, Lee J, Koh WG. **(Co-first author)**

*Bioact Mater.* 2022 Nov 29;23:383-393. doi: 10.1016/j.bioactmat.2022.11.010.

24. Retinal proteome analysis reveals a region-specific change in the rabbit myopia model.

Moon CE, **Ji YW**, Lee JK, Han K, Kim H, Byeon SH, Han S, Han J, Seo Y.

*Int J Mol Sci.* 2023 Jan 9;24(2):1286.

25. Integrated Analysis of Transcriptome and Proteome of the Human Cornea and Aqueous Humor Reveal Novel Biomarkers for Corneal Endothelial Cell Dysfunction.

Moon CE, Kim CH, Jung JH, Cho YJ, Choi KY, Han K, Seo KY, Lee HK, **Ji YW. (Co-corresponding author)**

*Int J Mol Sci.* 2023 Oct 19;24(20):15354.

26. Amplified fluorogenic immunoassay for early diagnosis and monitoring of Alzheimer's disease from tear fluid.

Lee S, Kim E, Moon CE, Park C, Lim JW, Baek M, Shin MK, Ki J, Cho H, **Ji YW**, Haam S. **(Co-corresponding author)**

*Nat Commun.* 2023 Dec 9;14(1):8153.